IJARAI

International Journal of
Advanced Research in Artificial Intelligence

Volume 5 Issue 11

www.ijarai.thesai.org

Editorial Preface

From the Desk of Managing Editor...

Artificial Intelligence is hardly a new idea. Human likenesses, with the ability to act as human, dates back to Geek mythology with Pygmalion's ivory statue or the bronze robot of Hephaestus. However, with innovations in the technological world, AI is undergoing a renaissance that is giving way to new channels of creativity.

The study and pursuit of creating artificial intelligence is more than designing a system that can beat grand masters at chess or win endless rounds of Jeopardy!. Instead, the journey of discovery has more real-life applications than could be expected. While it may seem like it is out of a science fiction novel, work in the field of AI can be used to perfect face recognition software or be used to design a fully functioning neural network.

At the International Journal of Advanced Research in Artificial Intelligence, we strive to disseminate proposals for new ways of looking at problems related to AI. This includes being able to provide demonstrations of effectiveness in this field. We also look for papers that have real-life applications complete with descriptions of scenarios, solutions, and in-depth evaluations of the techniques being utilized.

Our mission is to be one of the most respected publications in the field and engage in the ubiquitous spread of knowledge with effectiveness to a wide audience. It is why all of articles are open access and available view at any time.

IJARAI strives to include articles of both research and innovative applications of AI from all over the world. It is our goal to bring together researchers, professors, and students to share ideas, problems, and solution relating to artificial intelligence and application with its convergence strategies. We would like to express our gratitude to all authors, whose research results have been published in our journal, as well as our referees for their in-depth evaluations.

We hope that this journal will inspire and educate. For those who may be enticed to submit papers, thank you for sharing your wisdom.

Editorial Board

Reviewer Board Members

CONTENTS

Method for Aerosol Parameter Estimation Error Analysis - Consideration of Noises Included in the Measured Solar Direct and Diffuse Irradiance

Kohei Arai [1]

1 Graduate School of Science and Engineering
Saga University
Saga City, Japan

Abstract—**Method for error analysis of aerosol parameter estimation with assumed noises which are included in the measured solar direct and diffuse irradiance is proposed. The noises included in the measured solar direct and diffuse irradiance are assumed to be Chi-Square probability density function due to the fact that the measured irradiance is represented as output power which is square of output voltage which corresponds to the measured irradiance which is assumed to be normal distribution of probability density function. Aerosol parameters (refractive index which consists of real and imaginary parts, size distribution which is represented by Junge parameter) are estimated with the measured solar direct and diffuse irradiance which corresponds to the acquired output power of the measuring instrument which allows measurement of solar direct and diffuse irradiance. Through experiments with the measured solar direct and diffuse irradiance, it is found that the estimation accuracy of imaginary part of aerosol refractive index is the most sensitive to the added noises followed by size distribution of Junge parameter and real part of aerosol refractive index.**

Keywords—Aerosol; Atmospheric optical depth; Solar irradiance; Solar direct; Solar diffuse; Aereole; Junge parameter; Size distribution; Real and imaginary parts of refractive index

I. INTRODUCTION

The largest uncertainty in estimation of the effects of atmospheric aerosols on climate systems is from uncertainties in the determination of their microphysical properties, including the aerosol complex index of refraction that in turn determines their optical properties. The methods, which allow estimation of refractive indices, have being proposed so far [1]-[3].

Most of the methods use ground based direct, diffuse and aureole measurement data such as AERONET [4] and SKYNET [5]. The methodology for estimation of a complete set of vertically resolved aerosol size distribution and refractive index data, yielding the vertical distribution of aerosol optical properties required for the determination of aerosol-induced radiative flux changes is proposed [6].

The method based on the optical constants determined from the radiative transfer models of the atmosphere is also proposed [7]. Laboratory based refractive indices estimation methods with spectral extinction measurements are proposed

[8], [9]. All these existing methods are based on radiance from the sun and the atmosphere.

Through atmospheric optical depth measurements with a variety of relatively transparent wavelength, it is possible to estimate size distribution, molecule scattering, gaseous transmission, ozone and water vapor absorptions, etc. so that refractive index might be estimated [10]-[14]. In order to assess the estimation accuracy of refractive index with the proposed method, sensitivity analysis is conducted with a variety of parameters of the atmosphere. In particular, observation angle dependency is critical for atmospheric optical depth measurements. Therefore, it is conducted to assess influences due to observation angle on estimation accuracies of refractive index and size distribution. Similar researches are conducted and well reported [15]-[27].

The next section describes the proposed system followed by experiment. Then concluding remarks are described with some discussions.

II. PROPOSED METHOD

A. Radiative Transfer Function

Measured solar direct irradiance F on the ground is expressed in equation (1)

$$F = F_0 e^{-m_0 \tau_i} \tag{1}$$

where F_0 denotes extraterrestrial solar flux, m_0 denotes air-mass which can be represented as $1/\cos(\theta)$ where Θ denotes solar zenith angle, and τ_t denotes atmospheric optical depth which can be expressed in equation (2)

$$\tau_t = \tau_a + \tau_m = \tau_{as} + \tau_{aa} + \tau_{ms} + \tau_{ma} \tag{2}$$

where the first suffix t, a and m denotes total atmosphere, aerosols and molecules, respectively while the second suffix a and s denotes absorption and scattering, respectively. F can be measured on the ground while F_0 is well modeled by many researchers. On the other hand, m_0 can be well determined which results in estimation of atmospheric optical depth. Atmospheric optical depth due to aerosol and molecule has to be estimated together with their absorption and scattering components.

Meanwhile, measured solar diffuse irradiance on the ground can be expressed in equation (3).

$$E(\theta_0, \varphi) = E(\vartheta) = F m_0 \Delta\Omega \{\omega \tau_t P(\vartheta) + q(\vartheta)\} \qquad (3)$$

where φ denotes the angle between solar azimuth and observation azimuth directions while ϑ denotes azimuth and elevation angles. There is the following relation between both angles,

$$\cos(\vartheta) = cos^2\theta_0 + sin^2\theta_0 cos\varphi \qquad (4)$$

$\Delta\Omega$ denotes solid angle of the solar diffuse measuring instrument while ω denotes single scattering albedo which can be represented as follows,

$$\omega = (\tau_{as} + \tau_{ms})/\tau_{t_k} \qquad (5)$$

$P(\vartheta)$ and $q(\vartheta)$ denotes scattering phase function and multiple scattering component, respectively. $P(\vartheta)$ is expressed as follows,

$$P(\vartheta) = \{\tau_{ms}P_m(\vartheta) + \tau_{as}P_a(\vartheta)\}/(\tau_{ms} + \tau_{as}) \qquad (6)$$

Because of the observation wavelength and molecule radius has the following relation,

$$\frac{\pi r_a}{\lambda} < 0.4 \qquad (7)$$

molecule component of scattering can be expressed based on the Rayleigh scattering theory. Molecule component of scattering phase function $P_m(\vartheta)$ can be expressed as follows,

$$P_m(\vartheta) = \left(\frac{3}{4}\right)(1 + cos^2\vartheta) \qquad (8)$$

Molecule scattering component of the atmospheric optical depth is represented as follows,

$$\tau_{ms} =$$
$$\{0.008569\lambda^{-4}(1 + 0.0113\lambda^{-2} + 0.00013\lambda^{-4})\}\left(\frac{p}{p_0}\right)\left(\frac{T_0}{T}\right) \quad (9)$$

where λ denotes observation wavelength while p and p_0 denotes atmospheric pressure on the ground, standard atmospheric pressure (1013.25 hPa), respectively. On the other hand, T_0 and T denotes standard air-temperature on the ground (288.15 K) and air-temperature on the ground, respectively.

Meanwhile, observation wavelength and aerosol particle size has the following relation,

$$0.4 < \frac{\pi r_a}{\lambda} < 3 \qquad (10)$$

Aerosol scattering is expressed based on the Mie scattering theory.

Aerosol scattering intensity is expressed as equation (11).

$$\beta_a(\vartheta) = \frac{r^2}{2\pi}\int_{r_{min}}^{r_{max}}\{i_1(\vartheta, x, \widetilde{m}) + i_2(\vartheta, x, \widetilde{m})\}n(r)dr \quad (11)$$

where i_1, i_2 denotes Mie scattering intensity function as the function of x of size parameter, ϑ, and $\widetilde{m}$ of aerosol refractive index. On the other hand, $n(r)$ denotes the number of aerosol particles of which the radius is r and is called as number of aerosol particle size distribution in unit of 1/cm²/μm.

$$n(r) = dN(r)/dr \qquad (12)$$

The size parameter can be represented as follows,

$$x = \left(\frac{2\pi}{\lambda}\right)r \qquad (13)$$

On the other hand, aerosol optical depth is represented as follows,

$$\tau_a = \int_{r_{min}}^{r_{max}}\pi r^2 Q_{ext}(x, \widetilde{m})n(r)dr \qquad (14)$$

where Q is called as Extinction Efficiency Factor. Sometime, the following volume scattering size distribution is used.

$$v(r) = \frac{vd}{d \ln r} \qquad (15)$$

There is the well-known relation between the number and volume of size distributions as follows,

$$v(r) = \frac{4}{3}\pi r^4 n(r) \qquad (16)$$

Junge proposed the following size distribution function with Junge parameter γ,

$$Cr^{-\gamma} = \frac{dn}{d \ln r} \qquad (17)$$

In this paper, the Junge function of size distribution is used because of its simplicity with only one Junge parameter.

Let integral kernel functions be

$$K_{ext}(x, \widetilde{m}) = \left(\frac{3}{4}\right)\frac{Q_{ext}(x,\widetilde{m})}{x}$$
$$K(\vartheta, x, \widetilde{m}) = \frac{3}{2}\frac{i_1(\vartheta,x,\widetilde{m}) + i_2(\vartheta,x,\widetilde{m})}{x^3} \qquad (18)$$

Then

$$\beta_a(\vartheta) = \frac{2\pi}{\lambda}\int_{r_{min}}^{r_{max}}K(\vartheta, x, \widetilde{m})v(r)\, d\ln r \qquad (19)$$

$$\tau_a = \frac{2\pi}{\lambda}\int_{r_{min}}^{r_{max}}K_{ext}(x, \widetilde{m})v(r)\, d\ln r \qquad (20)$$

$$P_a(\vartheta) = \beta_a(\vartheta)/\omega_a \tau_a \qquad (21)$$

Solar diffuse irradiance taking into account the multiple scattering in the atmosphere measured on the ground can be represented as follows,

$$L(\vartheta) = F_0 m_0 e^{-m\tau_t}\{(\tau_{ms} + \tau_{MS})P_m(\vartheta) + \tau_{as}P_a(\vartheta) + \tau_A P_m(0°)\} \qquad (22)$$

where $(\tau_{ms}P_m(\vartheta))$ implies Rayleigh scattering component while $(\tau_{MS})P_m(\vartheta)$ implies multiple scattering component in the atmosphere. On the other hand, $\tau_{as}P_a(\vartheta)$ implies aerosol scattering component while $\tau_A P_m(0°)$ implies multiple scattering component in the atmosphere after the reflection on the ground. Solar diffuse flux can be expressed as $L(\vartheta)$ multiplied by observation solid angle $\Delta\Omega$. Meanwhile, τ_{MS} and τ_A are expressed empirically as follows,

$$\tau_{MS} = 0.02\tau_{SS} + 1.2\tau_{SS}^2\mu_0^{\frac{-1}{4}} \qquad (23)$$

$$\tau_A = \frac{A\tau_2}{1 - A\tau_3} \qquad (24)$$

where

$$\tau_{SS} = \tau_{ms} + \tau_{sa}$$
$$\mu_0 = \cos(\theta_0)$$
$$\tau_2 = 1.34\tau_{SS}\mu_0\{1 + 0.22\left(\frac{\tau_{SS}}{\mu_0}\right)^2\}$$
$$\tau_3 = 0.9\tau_S - 0.92\tau_{SS}^2 + 0.54\tau_{SS}^3$$

Therefore, the contribution of multiple scattering in the atmosphere is expressed as follows,

$$q(\vartheta) = \tau_{MS}P_m(\vartheta) + \tau_A P_m(0°) \qquad (25)$$

B. Actual Radiative Transfer Equation Solving

The following much stable parameter is introduced,

$$R(\vartheta) = \frac{E(\vartheta)}{Fm_0\Delta\Omega} = \omega\tau_t P(\vartheta) + q(\vartheta) = \beta(\vartheta) + q(\vartheta) \quad (26)$$

Instead of $E(\vartheta)$, $R(\vartheta)$ does not have large influence due to calibration error of the measuring instrument for solar direct and diffuse irradiance. $\omega\tau_t P(\vartheta)$ is replaced to $\beta(\vartheta)$. It is called single scattering intensity. Widely used aerosol parameter estimation method and software code is called Skyrad.Pack developed by Teruyuki Nakajima [11]. In the Skyrad.Pack ver.4.2, iteration method is used as follows,

$$\beta_a^{(1)}(\vartheta) = R_{mean}(\vartheta)$$
$$\beta_a^{(n+1)}(\vartheta) = R_{mean}(\vartheta)\beta_a^{(n)}(\vartheta)\Big/ R^{(n)}(\vartheta)$$

where (n) denotes the iteration number while $R_{mean}(\vartheta)$ denotes the measured solar diffuse irradiance. This method is appropriate in the sense of optimization of single scattering albedo and flux, as well as contribution factor of the multiple scattering component. In order to estimated single scattering flux, we have to know aerosol refractive index and size distribution. Therefore, inverse problem solving method is needed for this. The proposed method uses Moore-Penrose generalized inverse matrix method. Volume vector v (r dimension) of unknown size distribution $v^{(n)}(r)$ is assumed to be the matrix g which consists of a measured aerosol scattering flux $\beta_a^{(n)}(\vartheta)$ and aerosol optical depth $\tau_a^{(n-1)}$. Then,

$$g = Gv + \varepsilon \quad (27)$$

where G denotes a linear multiple term matrix. Thus, the size distribution can be determined as follows,

$$v = (G^T G + \eta H)^{-1} A^T g \quad (28)$$

where H denotes a smoothing matrix while η denotes Lagrange multiplier.

C. Added Noise on the Measured Solar Direct and Diffuse Irradiance
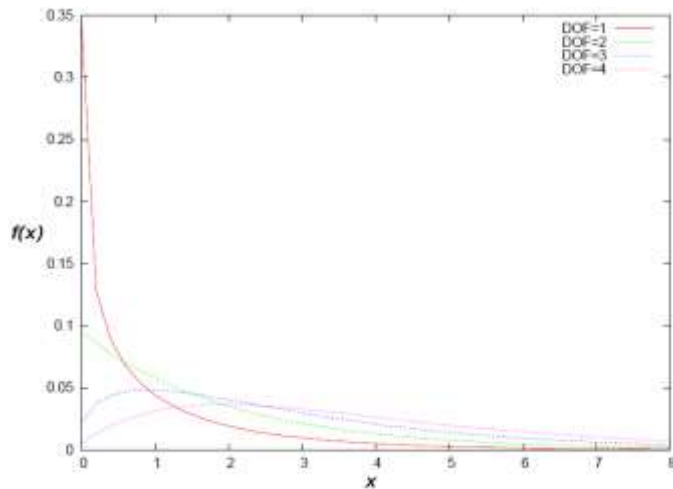
Fig. 1.   Examples of the Chi-Square probability density function

The output of the measuring instrument for solar direct and diffuse irradiance is represented as a power. The probability density function of the output noise voltage "x" of the instrument is assumed to be Normal distribution (Gaussian distribution). Therefore, the probability density function of the output noise power "x^2" of the instrument is assumed to be Chi-Square distribution. Examples of the Chi-Square probability density function $f(x)$ are shown in Fig.1.

Where DOF denotes Degree of Freedom of the parameter of Chi-Square probability density function.

III.   EXPERIMENTS

A. The Instrument and Data Used

POM-01 of sky-radiometer which allows measurements of solar direct and diffuse as well as aureole irradiance measurements is used. Fig.2 shows outlook and calibration coefficient as well as output power trends of the POM-01. POM-01 is set up on the top of the 7th building of the Science and Engineering Faculty of Saga University (1 Honjo, Saga, 840-8502 Japan). POM-01 measures solar direct irradiance with sun tracking capability and solar diffuse irradiance with 50 different diffuse angles in maximum with the following 7 center wavelength, 315, 400, 500, 675, 870, 940, 1020 nm. 315 nm is ozone absorption band while 940 nm is water absorption band, respectively.

(a) Outlook
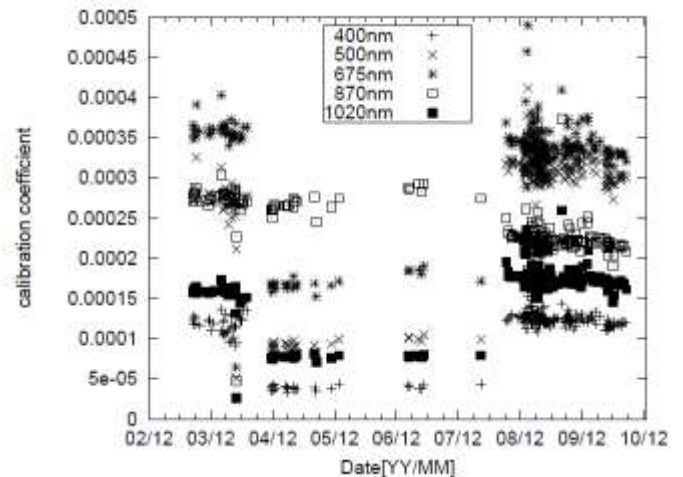
(b) Calibration coefficient
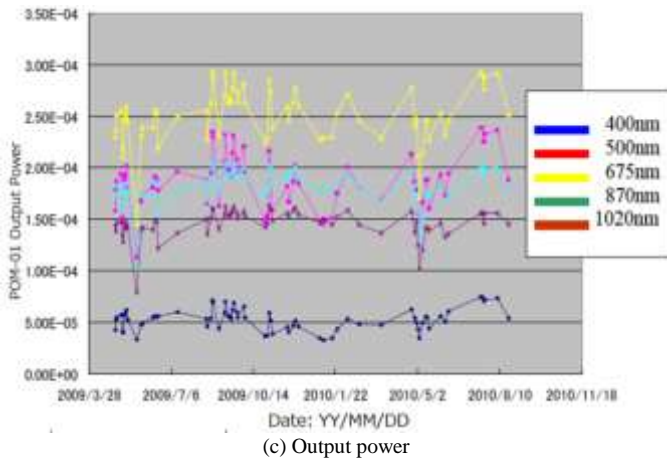
(c) Output power

Fig. 2. Outlook and calibration coefficient as well as output power trend of POM-01

(b) Solar diffuse

Fig. 3. Influence due to Chi-Square distributed additive noise on the output power of the measuring instrument for solar direct and diffuse irradiance

POM-01 has self-calibration function. Using the function, calibration data is acquired routinely. Calibration coefficient trend can be divided into three periods, March 2003 to July 2004, July 2004 to October 2008 and October to now.

Fine weather condition of sky-radiometer data which is measured at 11:08 in the morning on May 25 2009 in the third period is selected due to the fact that calibration coefficients in the third period are relatively stable.

B. The Preliminary Experiments

The measured data for both solar direct and diffuse irradiances are the output power of the measuring instrument in unit of [W]. Firstly, the measured output powers are plotted as a function of scattering angle with the different DOF (1,2,3,4) of the additive noise followed by the Chi-Square distribution in Fig.3. In this case, 100% of noise is added on the measured output power. In accordance with increasing of DOF, the output power of POM-01 is getting up as shown in Fig.3 (a). Meanwhile, the output power of POM-01 decreases in accordance with increasing of DOF as shown in Fig.3 (b).

On the other hand, skyrad.pack ver.4.2 allows estimation of volume spectral aerosol size distribution function. Using the relation between volume spectra and Junge size distribution function, equation (16), Junge parameter can be estimated based on the well-known least square method. Fig.4 shows the estimated Junge size distribution function for the aerosols on May 25 2009. It is found that the least square method does works for conversion from volume spectra to Junge distribution function with quit small error.

The skyrad.Pack ver.4.2 requires the parameter for conversion, the number of iterations (NLOOP). In order to determine the parameter, the residual error is calculated as a function of NLOOP for the data which is acquired on May 25 2009. Fig.5 shows the result. Fig.5 also shows the approximate function of residual errors which is expressed with the following function,

$$f(x) = ax^b \qquad (29)$$

where $a = 397.708$ and $b = -1.602$.

(a) Solar direct
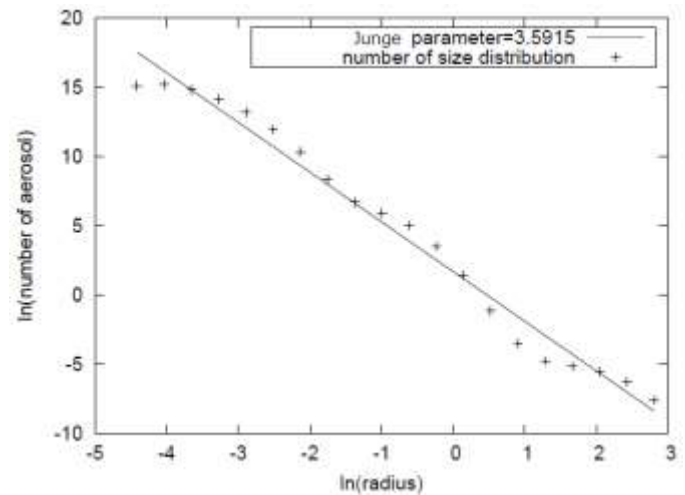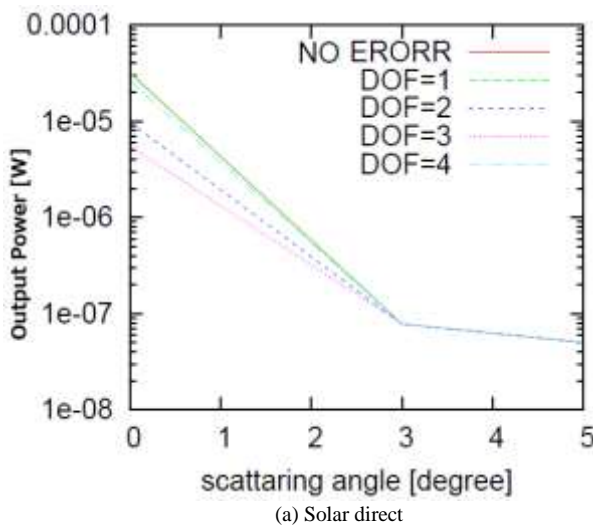
Fig. 4. Junge size distribution function of the aerosols on May 25 2009
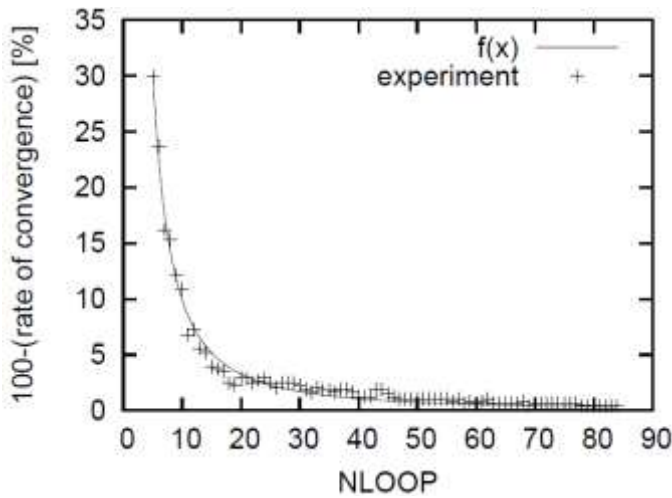
Fig. 5. Residual error (100-rate of conversgence) as the function of the number of iterations (NLOOP)

C. The Experimental Results

Using the modified skyrad.pack ver.4.2 described above, aerosol parameters, Real and Imaginary parts of aerosol refractive index and size distribution (Junge parameter) are estimated with the measured solar direct and diffuse irradiance which are measured with POM-01 on May 25 2009. Some of the errors are added on the solar direct angle and solar diffuse angle, respectively. On the other hand, Chi-Square distributed noises are added on the output power of the instrument. Thus sensitivities of the pointing angle error and added noise on the estimated aerosol parameters are clarified.

Fig.6 (a), (b) and (c) shows the solar direct pointing angle error on the estimated real part, imaginary part of refractive index and Junge parameter, respectively. The estimation error is evaluated with percent errors. As shown in Fig.6, it is easily found that the percent errors increase in accordance with increasing of solar direct pointing angle error. Also, it is found that the percent errors increase in accordance with decreasing of wavelength. Meanwhile, added noise influences are not so clear for the changing DOF of the Chi-Square distribution. Because of the influence due to the changing of DOF is not so clear in the Fig.6, two dimensional graphs are created. Fig.7 (a), (b), (c) and (d) shows the influence due to solar direct pointing angle error for the DOF is 1 to 4 on the estimated real part. The estimation error is evaluated with percent errors.

(a) Real part

(b) Imaginary part
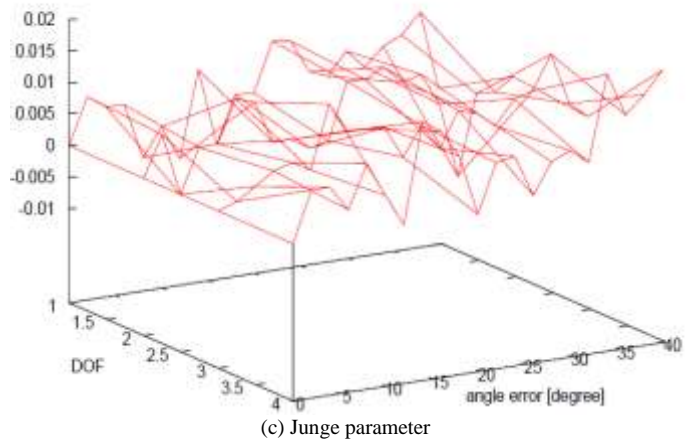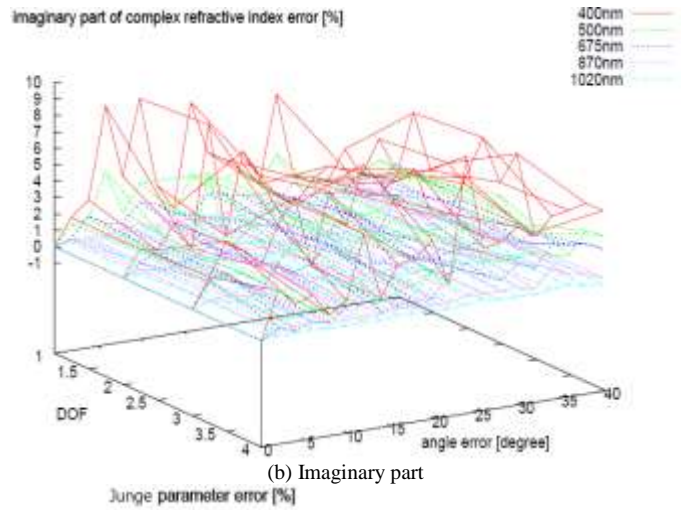
(c) Junge parameter

Fig. 6. Solar direct pointing angle error on the estimated real part, imaginary part of refractive index and Junge parameter

As shown in Fig.7, it is easily found that the percent errors increase in accordance with increasing of solar direct pointing angle error. Also, it is found that the percent errors increase in accordance with decreasing of wavelength.

(a) DOF=1

(b) DOF=2

(C) DOF=3

(d) DOF=4
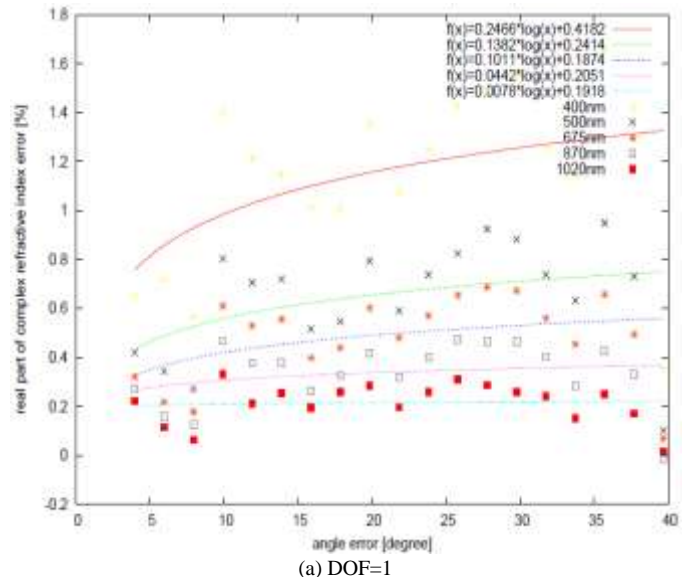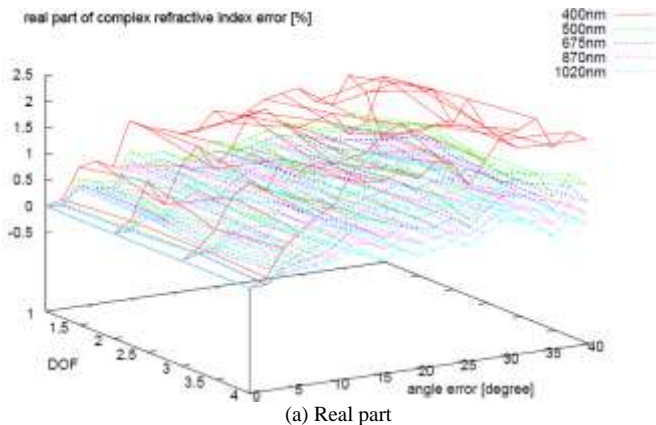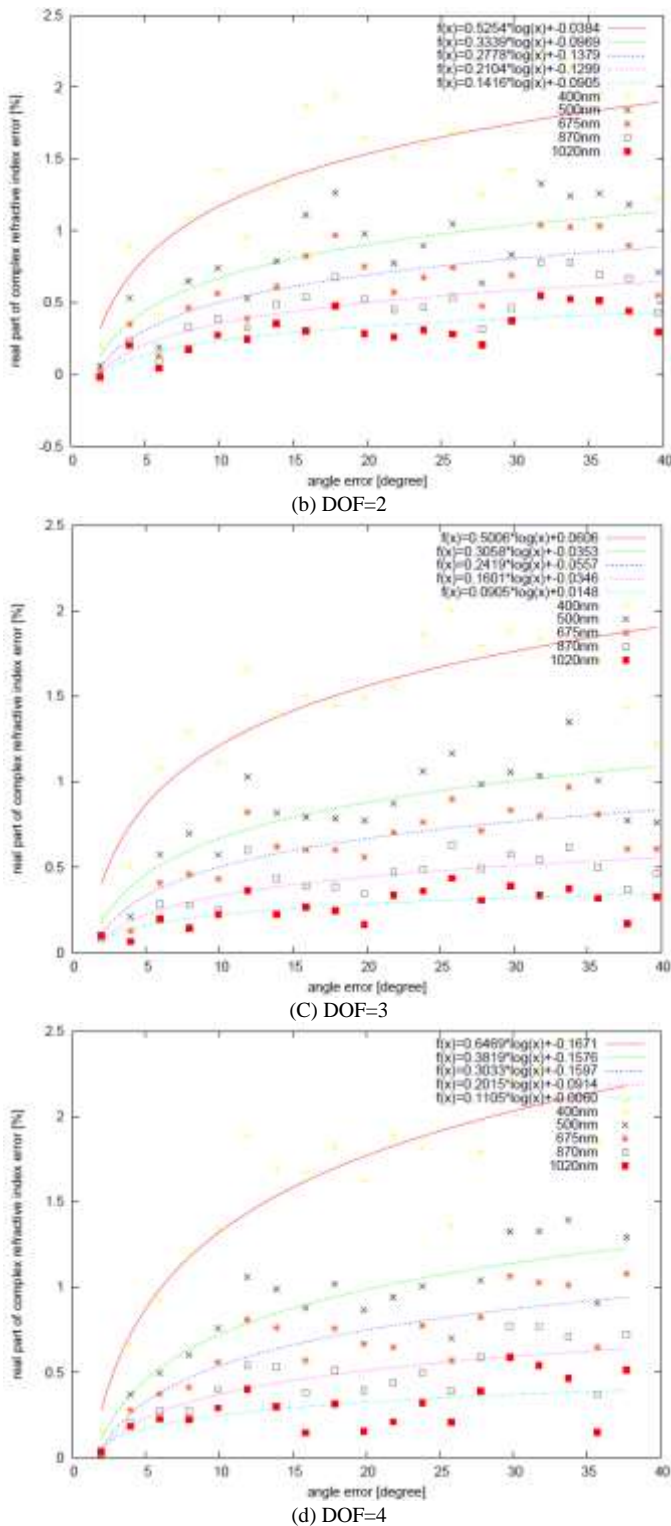
Fig. 7.   Influence due to solar direct pointing angle error for the DOF is 1 to 4 on the estimated real part

Fig.8 (a), (b) and (c) shows the solar diffuse pointing angle error on the estimated real part, imaginary part of refractive index and Junge parameter, respectively. The estimation error is evaluated with percent errors. As shown in Fig.8, it is easily found that the percent errors increase in accordance with

increasing of solar direct pointing angle error. Also, it is found that the percent errors increase in accordance with decreasing of wavelength. Meanwhile, added noise influences are not so clear for the changing DOF of the Chi-Square distribution.

Because of the influence due to the changing of DOF is not so clear in the Fig.8, two dimensional graphs are created. Fig.9 (a), (b), (c) and (d) shows the influence due to solar diffuse pointing angle error for the DOF is 1 to 4 on the estimated real part. The estimation error is evaluated with percent errors. As shown in Fig.9, it is easily found that the percent errors increase in accordance with increasing of solar diffuse pointing angle error. Also, it is found that the percent errors increase in accordance with decreasing of wavelength.

(a) Real part

(b) Imaginary part
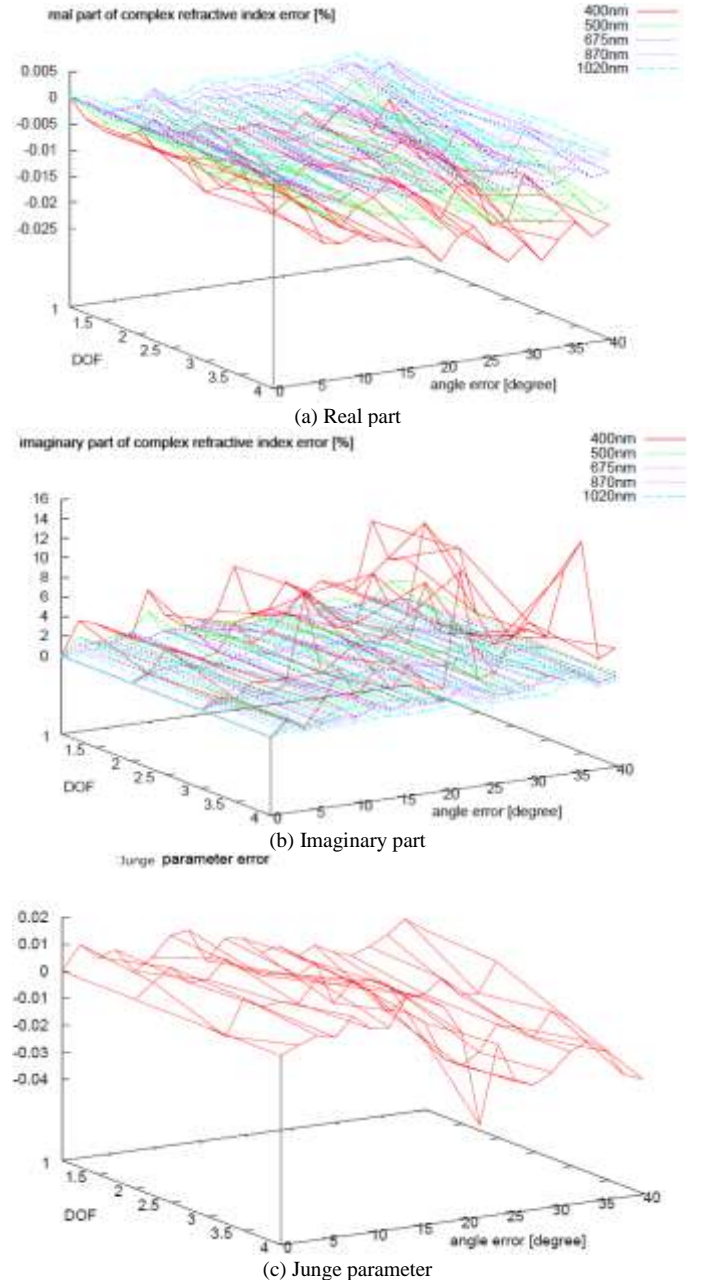
(c) Junge parameter

Fig. 8.   Solar diffuse pointing angle error on the estimated real part, imaginary part of refractive index and Junge parameter

(a) DOF=1
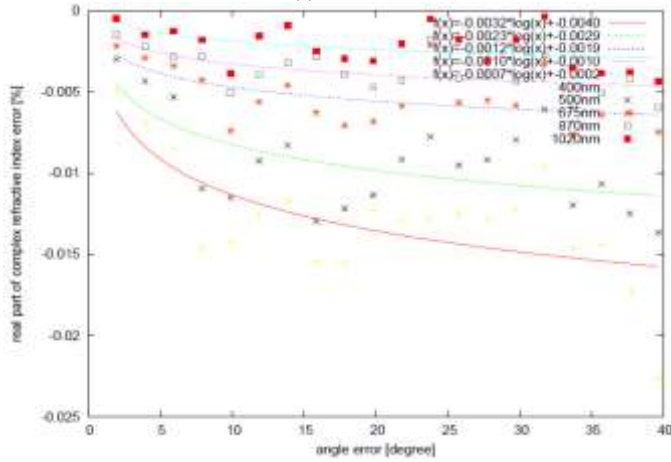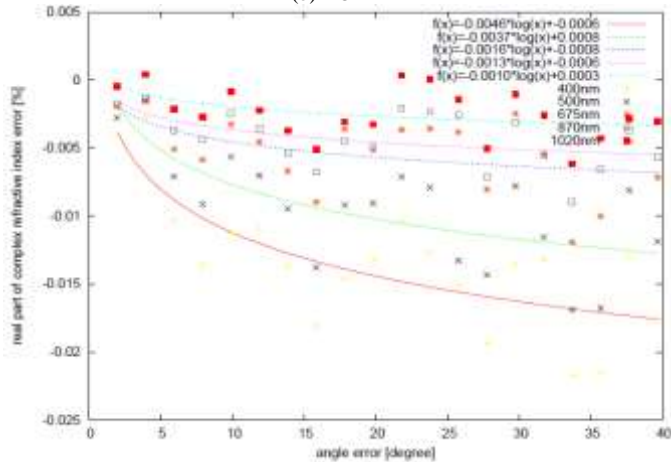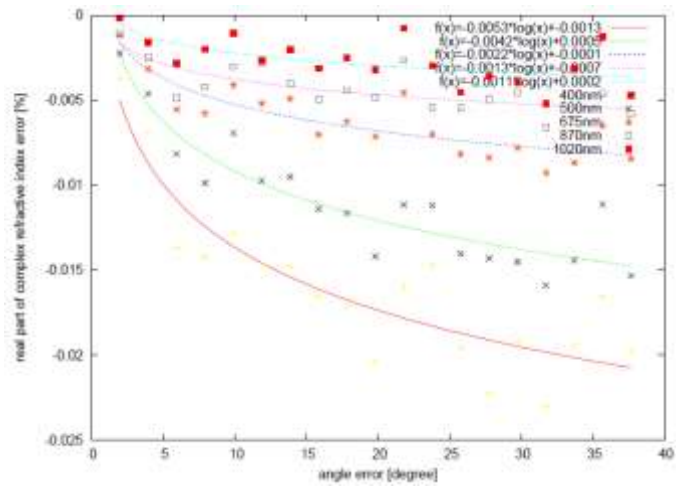
(d) DOF=4

Fig. 9. Influence due to solar diffuse pointing angle error for the DOF is 1 to 4 on the estimated real part

IV. CONCLUSION

Through the experiments for investigation of influence due to Chi-Square distributed additive noises included in the measured solar direct and diffuse irradiance on estimations of aerosol refractive index and size distribution, it is found that the influence is getting increased according to shortening of the wavelength and is decreasing in accordance with increasing of DOF of Chi-Square probability density function.

When the Chi-Square noises are added to the solar direct irradiance, the estimation error of real part of refractive index is getting large in accordance with increasing of solar direct pointing angle errors because of aerosol scattering factor is over estimated. Also, the estimation error of imaginary part of refractive index is increased with increasing of solar direct pointing angle errors. The influence on imaginary part of refractive index is much significant in comparison to the influence of real part of refractive index due to the fact that the absolute value of the imaginary part of refractive index is much smaller than that of real part of refractive index. The estimation error of real part of refractive index is well approximated with solar direct pointing angle error. All these influence is increased with shortening of the measuring wavelength due to the fact that the influence depends on aerosol optical depth (aerosol optical depth is increased with shortening of the measured wavelength. On the other hand, the influence of solar direct pointing angle error does not depend on the Chi-Square distributed noises of the solar direct irradiance. This is because that there is less sensitive to the solar direct irradiance.

(b) DOF=2

(c) DOF=3

The estimation error of imaginary refractive index is increased with increasing of the solar diffuse pointing angle error. This is because that aerosol scattering factor is underestimated due to decreasing of solar diffuse irradiance. Also, the estimation error of Junge parameter is decreased with increasing of solar diffuse pointing angle error. The influence of imaginary part of refractive index is greater than that of real part of refractive index due to the fact that size distribution is much sensitive to imaginary part of refractive index comparing to that of real part of refractive index.

Meanwhile, it is found that overall RMSE of real part of refractive index estimations over the experimental conditions is 0.0261 in maximum while that of imaginary part of refractive index is 0.00919 in maximum. On the other hand, overall RMSE of aerosol size distribution of Junge parameter estimations over the experimental conditions is 0.230 in maximum.

The proposed method for error analysis on aerosol parameter estimation influenced by existing noise included in the measured solar direct and diffuse irradiance which is accordance with Chi square probability density function is validated. Further investigation is required for appropriateness of the assumed Chi square probability density function of included noise.

REFERENCES

[1] Shaw, G.E., Error analysis of multi-wavelength sunphotometry. Pure Appl. Geophys., 114, 1, 1976.

[2] Hoppel, W. A., J. W. Fitzgerald, G. M. Frick, R. E. Larson, and E. J. Mack, Aerosol size distributions and optical properties found in the marine boundary layer over the Atlantic Ocean, J. Geophys. Res., 95, 3659-3686, 1990.

[3] Holben, B. N., et al., AERONET- A federated instrument network and data achieve for aerosol characterization, Remote Sens., 12, 1147-1163, 1991.

[4] Holben, B.N., and Coauthors, AERONET-A federated instrument network and data archive for aerosol characterization. Remote Sens. Environ., 66, 1-16. 1998.

[5] Aoki, K., T. Takamura, and T. Nakajima, Aerosol optical properties measured by SKYNET sky radiometer validation network. Proc. of the 2nd EarthCARE Workshop, 133-134, 2005.

[6] Redemann, R. P. Turco, K. N. Liou, P. B. Russell, R. W. Bergstrom, B. Schmid, J. M. Livingston, P. V. Hobbs, W. S. Hartley, S. Ismail, R. A Ferrare, E. V. Browell, Retrieving the vertical structure of the effective aerosol complex index of refraction from a combination of aerosol in situ and remote sensing measurements during TARFOX, J. Geophys. Res., 105, D8, 9949–9970, 2000.

[7] M.L.Clapp, and R.E.Miller, Complex Refractive Indices of Crystalline Hydrazine from Aerosol Extinction Spectra, Icarus, 23, 2, 396-403(8), 1996.

[8] R. Eiden, Determination of the complex index of refraction of spherical aerosol particles, Appl. Opt. 10, 749-757, 1971.

[9] G. E. Thomas, S. F. Bass, R. G. Grainger, and A. Lambert, Retrieval of aerosol refractive index from extinction spectra with a damped harmonic-oscillator band model, Appl. Opt. 44, 1332-1341, 2005.

[10] Kohei Arai, Aerosol refractive index retrievals with atmospheric polarization measuring data, Proceedings of the SPIE, 7461-06, 1-9, 2009

[11] Teruyuki Nakajima, et al., Use of sky brightness measurements from ground for remote sensing of particulate polydispersions, Applied Optics, Vol.35 No..15 pp.2672-2686 May 1996.

[12] Teruyuki Nakajima, et al., Retrieval of the optical properties of aerosols from aureole and extinction data, Applied Optics, Vol.22 No..19 pp.2951-2959 October 1983.

[13] M. A. Box and A. Deepak, An Approximation to Multiple Scattering in the Earth's Atmo-sphere:Almucanter Radiance Formulation, J. Atmos. Sci. Vol38 pp.1037-1048 1981.

[14] Mitsugu Toriumi, Hideaki Takenaka, Tadashi Kato, Toshikazu Hasegawa, Takashi Nakajima, Tamio Takamura and Teruyuki Nakajima: Estimation of Aerosol Optical Thickness by PAR Radiometer, Journal of The Remote Sensing Society of Japan, 30, 2, pp.81-89, 2010 .

[15] Tsutomu Takashima, Kazuhiko Masuda, Kohei Arai, Satoshi Tsuchida, Observation of Optical Property of the Atmosphere in Particular Aerosols at Deserted Areas In USA Using Sun-photometer and Polarization Spectrometer, Journal of Remote Sensing Society of Japan, Vol.20, No.3, pp.47-60, (2000).

[16] Kohei Arai, Influence of Non-Spherical Sea Salt Aerosol Particles Containing Bubbles on the Top of the Atmosphere Radiance, Journal of Remote Sensing Society of Japan, Vol.20, No.5, pp.32-39, (2001).

[17] Kohei Arai, Tatsuya Kawaguchi, Adjucency Effect of Layered Clouds taking Into Account Phase Function of Cloud Particles and Multi-Layered Plane Parallel Atmosphere Based on Monte Carlo Method, Journal of Japan Society of Photogrammetry and Remote Sensing, Vol.40, No.6, 2001.

[18] Kohei Arai, Yoko Takamatsu, Influence of Spume Aerosol Particles on the Top of the Atmosphere Radiance, Journal of Remote Sensing Society of Japan, Vol.23, No.4, pp.355-363, 2003.

[19] Kohei Arai, Xing Ming Liang, Estimation of Method for the Top of the Atmosphere Radiance Taking Into Account Polarized Up-welling and Down-welling Radiance, Journal of Japan Society of Photogrammetry and Remote Sensing, 44,3, 4-12,(2005)

[20] K.Arai, Monte Carlo simulation of polarized atmospheric irradiance for determination of refractive index of aerosols, International Journal of Research and Review on Computer Science, 3, 4, 1744-1748, 2012.

[21] K.Arai, Monte Carlo ray tracing based sensitivity analysis of the atmospheric and oceanic parameters on the top of the atmosphere radiance, International Journal of Advanced Computer Science and Applications, 3, 12, 7-13, 2012.

[22] K.Arai, Monte Carlo ray tracing based sensitivity analysis of the atmospheric and oceanic parameters on the top of the atmosphere radiance, International Journal of Advanced Computer Science and Applications, 3, 12, 7-13, 2012.

[23] Kohei Arai, Method for estimation of aerosol parameters based on ground based atmospheric polarization irradiance measurements, International Journal of Advanced Computer Science and Applications, 4, 2, 226-233, 2013.

[24] Kohei Arai, Sensitivity analysis and validation of refractive index estimation method with ground based atmospheric polarized radiance measurement data, International Journal of Advanced Computer Science and Applications, 4, 3, 1-6, 2013.

[25] Kohei Arai, Sensitivity analysis for aerosol refractive index and size distribution estimation methods based on polarized atmospheric irradiance measurements, International Journal of Advanced Research in Artificial Intelligence, 3, 1, 16-23, 2014.

[26] K.Arai, Vicarious calibration data screening method based on variance of surface reflectance and atmospheric optical depth together with cross calibration, International Journal of Advanced Research on Artificial Intelligence, 4, 11, 1-8, 2015.

[27] K.Arai, Kenta Azuma, Method for surface reflectance estimation with MODIS by means of bi-section between MODIS and estimated radiance as well as atmospheric correction with sky-radiometer, International Journal of Advanced Research on Artificial Intelligence, 4, 11, 8-15, 2015.

AUTHORS PROFILE

Kohei Arai, He received BS, MS and PhD degrees in 1972, 1974 and 1982, respectively. He was with The Institute for Industrial Science and Technology of the University of Tokyo from April 1974 to December 1978 and also was with National Space Development Agency of Japan from January, 1979 to March, 1990. During from 1985 to 1987, he was with Canada Centre for Remote Sensing as a Post-Doctoral Fellow of National Science and Engineering Research Council of Canada. He moved to Saga University as a Professor in Department of Information Science on April 1990. He was a counselor for the Aeronautics and Space related to the Technology Committee of the Ministry of Science and Technology during from 1998 to 2000. He was a councilor of Saga University for 2002 and 2003. He also was an executive councilor for the Remote Sensing Society of Japan for 2003 to 2005. He is an Adjunct Professor of University of Arizona, USA since 1998. He also is Vice Chairman of the Commission-A of ICSU/COSPAR since 2008. He received Science and Engineering Award of the year 2014 from the minister of the ministry of Science Education of Japan and also received the Bset Paper Award of the year 2012 of IJACSA from Science and Information Organization: SAI. In 2016, he also received Vikram Sarabhai Medal of ICSU/COSPAR and also received 20 awards. He wrote 34 books and published 520 journal papers. He is Editor-in-Chief of International Journal of Advanced Computer Science and Applications as well as International Journal of Intelligent Systsems and Applications. http://teagis.ip.is.saga-u.ac.jp/

Aerosol Parameter Estimation Method Utilizing Solar Direct and Diffuse Irradiance Measuring Instrument without Sun Tracking Mechanics

Kohei Arai [1]

1 Graduate School of Science and Engineering
Saga University
Saga City, Japan

Abstract—**Estimation method of aerosol parameter by means of solar direct and diffuse irradiance measurements with the proposed instrument of fiber-ball radiometer without sun tracking mechanics is proposed. Sky-radiometer and aureole-meter is well known instrument which allows measurements of solar direct and diffuse irradiance for estimation of aerosol parameter. The proposed fiber-ball radiometer also allows solar direct and diffuse irradiance measurements and is comparatively light as well as is composed without any mechanics so that it is portable and is enable to bring anywhere you want including test sites for field campaigns. Meanwhile, it is not always that the fiber-ball instrument points to the sun due to the error of the sun ephemeris calculations as well as sun track do not match to the actual one. Influence due to pointing error on aerosol parameter estimation error is clarified. Possible maximum pointing error may cause some error on aerosol parameter estimation. Experimental results show that 0.43%, 42.23%, 2.12% root mean square errors are suspected for real and imaginary part of refractive index and Junge parameter as of 1.747, 0.0056 and 3.0 of typical case of atmosphere.**

Keywords—*Aerosol; Atmospheric optical depth; Solar irradiance; Solar direct; Solar diffuse; Aereole; Junge parameter; Size distribution; Real and imaginary parts of refractive index*

I. INTRODUCTION

The largest uncertainty in estimation of the effects of atmospheric aerosols on climate systems is from uncertainties in the determination of their microphysical properties, including the aerosol complex index of refraction that in turn determines their optical properties. The methods, which allow estimation of refractive indices, have being proposed so far [1]-[3].

Most of the methods use ground based direct, diffuse and aureole measurement data such as AERONET [4] and SKYNET [5]. The methodology for estimation of a complete set of vertically resolved aerosol size distribution and refractive index data, yielding the vertical distribution of aerosol optical properties required for the determination of aerosol-induced radiative flux changes is proposed [6].

The method based on the optical constants determined from the radiative transfer models of the atmosphere is also proposed [7]. Laboratory based refractive indices estimation methods with spectral extinction measurements are proposed

[8], [9]. All these existing methods are based on radiance from the sun and the atmosphere.

Through atmospheric optical depth measurements with a variety of relatively transparent wavelength, it is possible to estimate size distribution, molecule scattering, gaseous transmission, ozone and water vapor absorptions, etc. so that refractive index might be estimated [10]-[14]. In order to assess the estimation accuracy of refractive index with the proposed method, sensitivity analysis is conducted with a variety of parameters of the atmosphere. In particular, observation angle dependency is critical for atmospheric optical depth measurements. Therefore, it is conducted to assess influences due to observation angle on estimation accuracies of refractive index and size distribution. Similar researches are conducted and well reported [15]-[27].

Most of measuring instruments which allows solar direct and diffuse irradiance measurements has sun tracking mechanics of which some malfunctions may occur sometime and it requires not so short time for collecting data of solar direct and diffuse irradiance. In order to overcome such problems, a new type of spectral radiometer without sun tracking mechanics is proposed here.

The next section describes the proposed system followed by experiment. The experiments are intended to show the sensitivity of solar direct and diffuse pointing angle on the aerosol parameter estimations. Then concluding remarks are described with some discussions.

II. PROPOSED METHOD

A. Conventional Method for Aerosol Parameter Estimation

Conventional method for aerosol parameter estimation is based on radiative transfer equation with measured solar direct and diffuse irradiance from the ground. The radiative transfer equation represents relation between solar direct and diffuse irradiance as well as aerosol parameters, refractive index and size distribution. Therefore, it is important to measure the solar direct and diffuse irradiance precisely. It usually requires solar tracking capability. Sun ephemeris can be calculated with the location and time information. Once the sun is acquired, the sun is tracked automatically. One of the solar direct and diffuse irradiance measuring instruments is shown in Fig.1. This is called as SkyRadiometer POM-01

manufactured by Prede Co. Ltd in Japan. Top left in Fig.1, there are two optics. One is for optical entrance of the radiometer while the other one is for sun tracker. Solar direct, Aureole, Diffuse irradiance can be measured with the main radiometer through the optical entrance. It covers ultra violet to near infrared wavelength. 315, 400, 500, 675, 870, 940 and 1020 nm is center wavelength of the radiometer. 315 nm is for ozone absorption band while 940 nm is for water vapor absorption band. Other five bands are transparent bands. In other word, atmospheric optical depth for these five bands is very thin. Using these two band data, column ozone and column water vapor is estimated. Major specification of the POM-01 is shown in Table 1.

Fig. 1.   Outlook of POM-01

TABLE I.   MAJOR SPECIFICATION OF POM-01

Field_of_view	0.5°
Minimum_scattering_angle	3°
Wavelength	315,400,500,675,870,940,1020nm
Band_Selection	Filter_Wheel
Detector	Silicon_Photo_Diode
Measurable_Range	2.5mA,250µA,25µA,250nA,25nA,2.5nA
Drive_System	Pulse_Motor
Measuring_Interval	Air-mass
Scan_Direction	Horizontal/Vertical_Directions
Measurable_Scattering_Angle	50

Response time is not so fast. It requires not so short time for measurement of solar direct and 50 points of diffuse irradiance. During the measurement, the atmosphere may change. Due to the fact that the sun tracking needs mechanics. Therefore, undesirable malfunction occurs sometime. The proposed system is developed to overcome such that problems. Namely, solar direct and diffuse irradiance measuring instrument without sun tracking mechanics is proposed here.

B. Proposed Method for Aerosol Parameter Estimation

The proposed method for aerosol parameter estimation is ased on radiative transfer equation with measured solar direct and diffuse irradiance which is acquired by the measuring instrument of the irradiance without sun tracker. Fundamental spectral-radiometer is based on the existing commercially available spectral-radiometer of MS-720 manufactured by Eiko Co. Ltd. Outlook and major specification is shown in Fig.2 and Table 2, respectively. MS-720 is the portable type of spectral-radiometer of which the wavelength coverage from ultra-violet to near infrared (350-1050nm) with the Zeiss grating element and silicon photo diode array of 256 channels. Spectral radiant flux can be measured with this MS-720. Wavelength interval is 3.3 nm while ± 5% of detector temperature correction can be done with this MS-720. Aperture angle (180, 90, 10 degrees) can be changed with attachment of the optical entrance.

Fig. 2.   Outlook of MS-720

TABLE II.   MAJOR SPECIFICATION OF MS-720

Wavelength_Coverage	350～1,050nm
Wavelength_Interval	3.3nm
Wavelength_Resolution	10nm
Wavelength_Accuracy	<0.3nm
Full_Aperture	180°
StrayLight	<0.15%
Temperature_Dependency	±5%
Output_Unit	W/m2/µm_or_µmol/m2/s/µm
Measuring_Interval	0.005～5sec(Automatic adjustment)

Replacing the optical entrance to the proposed fiber ball, every 32 second of solar direct and diffuse irradiance can be measured. The aperture angle is set at 32 second which corresponds to the viewing angle of the sun. Outlook of the proposed system for measurement of solar direct and diffuse irradiance is shown in Fig.3 (a). At the top of Fig.3, there is the fiber ball with a number of holes. The holes are optical entrance of the optical guide of optical fibers. The guided lights are input to the MS-720 through attachment at the optical entrance. Illustrative view of the fiber ball is shown in Fig.3 (b) while the configuration of the proposed measuring instrument with fiber ball and MS-720 of radiometer is illustrated in Fig.3 (c). On the other hand, the dimension of the fiber ball radiometer is illustrated in Fig.3 (d). The number of

holes of the fiber ball is 512 for the hemisphere. One of the problems of the proposed fiber ball is solar direct and diffuse angle pointing accuracy. The difference between sun ephemeris and pointing whole location of the fiber ball would be a problem.

The diameter of the fiber ball is just 5 cm. The hole size is 32 second in diameter which corresponds to 1.1mm. On the other hand, the diameter of the fiber is 20 micro-meter. Loss of the optical fiber is negligible because the length of the fiber is very short between the tip of the hole of the fiber ball and optical entrance of the MS-720 as shown in Fig.3 (c). The guided light is input to the grating of beam splitter and then the splitter light is guided to the two dimensional CCD array with 20000 of elements.

(a) Outlook
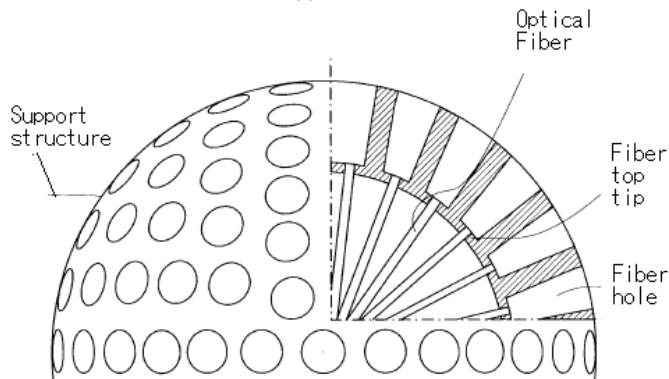
(b) Fiber ball
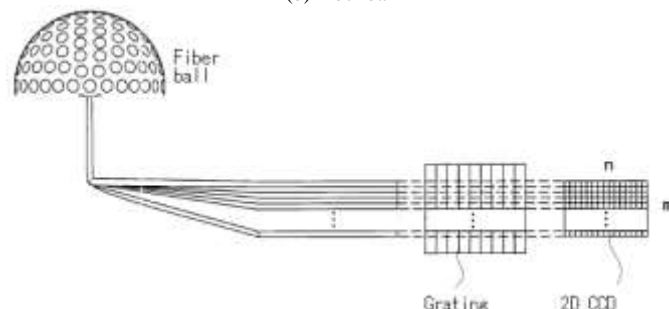
(c) Configuration of the proposed measuring instrument with fiber ball and MS-720 of radiometer
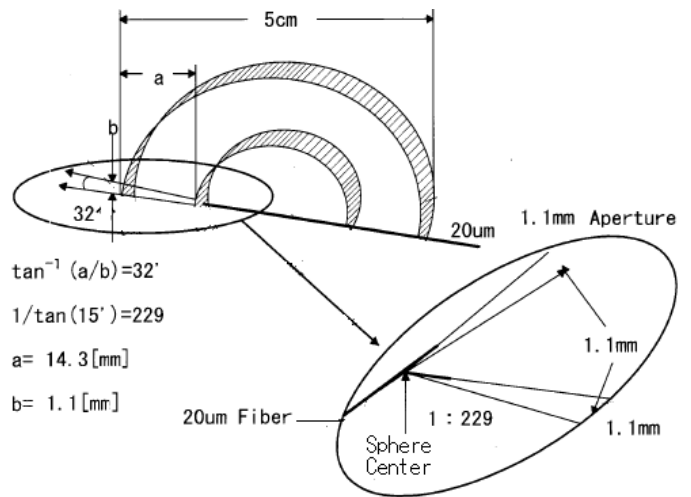
(d) Dimension of the fiber ball radiometer

Fig. 3. (a) Optical Fiber guided sky-radiometer, (b) fiber ball and (c) configuration of instrument. (d) Dimension of the fiber ball radiometer

C. Radiative Transfer Equation

Measured solar direct irradiance F on the ground is expressed in equation (1)

$$F = F_0 e^{-m_0 \tau_i} \tag{1}$$

where F_0 denotes extraterrestrial solar flux, m_0 denotes air-mass which can be represented as $1/\cos(\theta)$ where Θ denotes solar zenith angle, and τ_t denotes atmospheric optical depth which can be expressed in equation (2)

$$\tau_t = \tau_a + \tau_m = \tau_{as} + \tau_{aa} + \tau_{ms} + \tau_{ma} \tag{2}$$

where the first suffix t, a and m denotes total atmosphere, aerosols and molecules, respectively while the second suffix a and s denotes absorption and scattering, respectively. F can be measured on the ground while F_0 is well modeled by many researchers. On the other hand, m_0 can be well determined which results in estimation of atmospheric optical depth. Atmospheric optical depth due to aerosol and molecule has to be estimated together with their absorption and scattering components.

Meanwhile, measured solar diffuse irradiance on the ground can be expressed in equation (3).

$$E(\theta_0, \varphi) = E(\vartheta) = F m_0 \Delta \Omega \{ \omega \tau_t P(\vartheta) + q(\vartheta) \} \tag{3}$$

where φ denotes the angle between solar azimuth and observation azimuth directions while ϑ denotes azimuth and elevation angles. There is the following relation between both angles,

$$\cos(\vartheta) = \cos^2 \theta_0 + \sin^2 \theta_0 \cos\varphi \tag{4}$$

$\Delta\Omega$ denotes solid angle of the solar diffuse measuring instrument while ω denotes single scattering albedo which can be represented as follows,

$$\omega = (\tau_{as} + \tau_{ms})/\tau_{t_k} \tag{5}$$

$P(\vartheta)$ and $q(\vartheta)$ denotes scattering phase function and multiple scattering component, respectively. $P(\vartheta)$ is expressed as follows,

$$P(\vartheta) = \{\tau_{ms}P_m(\vartheta) + \tau_{as}P_a(\vartheta)\}/(\tau_{ms} + \tau_{as}) \quad (6)$$

Because of the observation wavelength and molecule radius has the following relation,

$$\frac{\pi r_a}{\lambda} < 0.4 \quad (7)$$

molecule component of scattering can be expressed based on the Rayleigh scattering theory. Molecule component of scattering phase function $P_m(\vartheta)$ can be expressed as follows,

$$P_m(\vartheta) = \left(\frac{3}{4}\right)(1 + cos^2\vartheta) \quad (8)$$

Molecule scattering component of the atmospheric optical depth is represented as follows,

$$\tau_{ms} = \{0.008569\lambda^{-4}(1 + 0.0113\lambda^{-2} + 0.00013\lambda^{-4})\}\left(\frac{p}{p_0}\right)\left(\frac{T_0}{T}\right) \quad (9)$$

where λ denotes observation wavelength while p and p_0 denotes atmospheric pressure on the ground, standard atmospheric pressure (1013.25 hPa), respectively. On the other hand, T_0 and T denotes standard air-temperature on the ground (288.15 K) and air-temperature on the ground, respectively.

Meanwhile, observation wavelength and aerosol particle size has the following relation,

$$0.4 < \frac{\pi r_a}{\lambda} < 3 \quad (10)$$

Aerosol scattering is expressed based on the Mie scattering theory.

Aerosol scattering intensity is expressed as equation (11).

$$\beta_a(\vartheta) = \frac{r^2}{2\pi}\int_{r_{min}}^{r_{max}}\{i_1(\vartheta,x,\widetilde{m}) + i_2(\vartheta,x,\widetilde{m})\}n(r)dr \quad (11)$$

where i1, i2 denotes Mie scattering intensity function as the function of x of size parameter, ϑ, and $\widetilde{m}$ of aerosol refractive index. On the other hand, $n(r)$ denotes the number of aerosol particles of which the radius is r and is called as number of aerosol particle size distribution in unit of $1/cm^2/\mu$m.

$$n(r) = dN(r)/dr \quad (12)$$

The size parameter can be represented as follows,

$$x = \left(\frac{2\pi}{\lambda}\right)r \quad (13)$$

On the other hand, aerosol optical depth is represented as follows,

$$\tau_a = \int_{r_{min}}^{r_{max}} \pi r^2 Q_{ext}(x,\widetilde{m})n(r)dr \quad (14)$$

where Q is called as Extinction Efficiency Factor. Sometime, the following volume scattering size distribution is used.

$$v(r) = \frac{vd}{d\ln r} \quad (15)$$

There is the well-known relation between the number and volume of size distributions as follows,

$$v(r) = \frac{4}{3}\pi r^4 n(r) \quad (16)$$

Junge proposed the following size distribution function with Junge parameter γ,

$$Cr^{-\gamma} = \frac{dn}{d\ln r} \quad (17)$$

In this paper, the Junge function of size distribution is used because of its simplicity with only one Junge parameter.

Let integral kernel functions be

$$K_{ext}(x,\widetilde{m}) = \left(\frac{3}{4}\right)\frac{Q_{ext}(x,\widetilde{m})}{x}$$
$$K(\vartheta,x,\widetilde{m}) = \frac{3}{2}\frac{i_1(\vartheta,x,\widetilde{m})+i_2(\vartheta,x,\widetilde{m})}{x^3} \quad (18)$$

Then

$$\beta_a(\vartheta) = \frac{2\pi}{\lambda}\int_{r_{min}}^{r_{max}} K(\vartheta,x,\widetilde{m})v(r)\,d\ln r \quad (19)$$

$$\tau_a = \frac{2\pi}{\lambda}\int_{r_{min}}^{r_{max}} K_{ext}(x,\widetilde{m})v(r)\,d\ln r \quad (20)$$

$$P_a(\vartheta) = \beta_a(\vartheta)/\omega_a\tau_a \quad (21)$$

Solar diffuse irradiance taking into account the multiple scattering in the atmosphere measured on the ground can be represented as follows,

$$L(\vartheta) = F_0 m_0 e^{-m\tau_t}\{(\tau_{ms} + \tau_{MS})P_m(\vartheta) + \tau_{as}P_a(\vartheta) + \tau_A P_m(0°)\} \quad (22)$$

where $(\tau_{ms}P_m(\vartheta))$ implies Rayleigh scattering component while $(\tau_{MS})P_m(\vartheta)$ implies multiple scattering component in the atmosphere. On the other hand, $\tau_{as}P_a(\vartheta)$ implies aerosol scattering component while $\tau_A P_m(0°)$ implies multiple scattering component in the atmosphere after the reflection on the ground. Solar diffuse flux can be expressed as $L(\vartheta)$ multiplied by observation solid angle $\Delta\Omega$. Meanwhile, τ_{MS} and τ_A are expressed empirically as follows,

$$\tau_{MS} = 0.02\tau_{SS} + 1.2\tau_{SS}^2\mu_0^{\frac{-1}{4}} \quad (23)$$

$$\tau_A = \frac{A\tau_2}{1-A\tau_3} \quad (24)$$

where

$$\tau_{SS} = \tau_{ms} + \tau_{sa}$$
$$\mu_0 = \cos(\theta_0)$$
$$\tau_2 = 1.34\tau_{SS}\mu_0\{1 + 0.22\left(\frac{\tau_{SS}}{\mu_0}\right)^2\}$$
$$\tau_3 = 0.9\tau_S - 0.92\tau_{SS}^2 + 0.54\tau_{SS}^3$$

Therefore, the contribution of multiple scattering in the atmosphere is expressed as follows,

$$q(\vartheta) = \tau_{MS}P_m(\vartheta) + \tau_A P_m(0°) \quad (25)$$

D. Actual Radiative Transfer Equation Solving

The following much stable parameter is introduced,

$$R(\vartheta) = \frac{E(\vartheta)}{Fm_0\Delta\Omega} = \omega\tau_t P(\vartheta) + q(\vartheta) = \beta(\vartheta) + q(\vartheta) \quad (26)$$

Instead of $E(\vartheta)$, $R(\vartheta)$ does not have large influence due to calibration error of the measuring instrument for solar direct and diffuse irradiance. $\omega\tau_t P(\vartheta)$ is replaced to $\beta(\vartheta)$. It is called single scattering intensity. Widely used aerosol parameter estimation method and software code is called Skyrad.Pack developed by Teruyuki Nakajima [11]. In the Skyrad.Pack ver.4.2, iteration method is used as follows,

$$\beta_a^{(1)}(\vartheta) = R_{mean}(\vartheta)$$

$$\beta_a^{(n+1)}(\vartheta) = R_{mean}(\vartheta) \beta_a^{(n)}(\vartheta) \Big/ R^{(n)}(\vartheta)$$

where (n) denotes the iteration number while $R_{mean}(\vartheta)$ denotes the measured solar diffuse irradiance. This method is appropriate in the sense of optimization of single scattering albedo and flux, as well as contribution factor of the multiple scattering component. In order to estimated single scattering flux, we have to know aerosol refractive index and size distribution. Therefore, inverse problem solving method is needed for this. The proposed method uses Moore-Penrose generalized inverse matrix method. Volume vector *v* (r dimension) of unknown size distribution $v^{(n)}(r)$ is assumed to be the matrix *g* which consists of a measured aerosol scattering flux $\beta_a^{(n)}(\vartheta)$ and aerosol optical depth $\tau_a^{(n-1)}$. Then,

$$g = Gv + \varepsilon \tag{27}$$

where *G* denotes a linear multiple term matrix. Thus, the size distribution can be determined as follows,

$$v = (G^T G + \eta H)^{-1} A^T g \tag{28}$$

where H denotes a smoothing matrix while η denotes Lagrange multiplier. Thus, aerosol parameters can be estimated with the measured solar direct and diffuse irradiance.

III. EXPERIMENTS

A. Preliminary Results

POM-01 has self-calibration function. Using the function, calibration data is acquired routinely. Calibration coefficient trend can be divided into three periods, March 2003 to July 2004, July 2004 to October 2008, and October to now. Calibration coefficient trend is shown in Fig.4. As shown in Fig.4, the calibration coefficients are relatively stable since October 2008. Therefore, a sensitivity analysis of the solar direct and diffuse pointing angle error on the aerosol parameter estimation is made for the period.

Fine weather condition of sky-radiometer data which is measured at 11:08 in the morning on May 25 2009 in the third period is selected due to the fact that calibration coefficients in the third period is relatively stable.
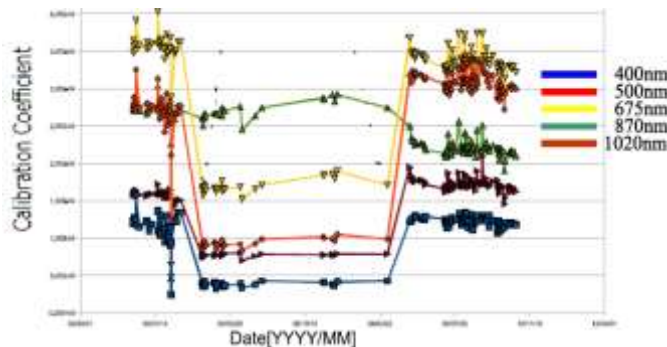
Fig. 4. Calibration coefficient trend of POM-01

B. Experimental Results

Using the modified skyrad.pack ver.4.2 described above, aerosol parameters, Real and Imaginary parts of aerosol refractive index and size distribution (Junge parameter) are estimated with the measured solar direct and diffuse irradiance which are measured with POM-01 on May 25 2009. Some of the errors are added on the solar direct angle and solar diffuse angle, respectively. Thus sensitivities of the pointing angle error on the estimated aerosol parameters are clarified.

Fig.5 (a) shows the solar direct pointing angle error on the estimated real part of refractive index while Fig.5 (b) shows that for imaginary part of refractive index, respectively. On the other hand, that for aerosol size distribution of Junge parameter is shown in Fig.5 (c). The estimation error is evaluated with Root Mean Square Error: RMSE and percent error. As shown in Fig.5, it is easily found that RMSE increases in accordance with increasing of solar direct pointing angle error. Also, it is found that RMSE increases in accordance with decreasing of wavelength.

On the other hand, Fig.6 shows the solar diffuse pointing angle error on the estimated real and imaginary parts of refractive index as well as Junge parameter. As shown in Fig.6, it is easily found that RMSE increases in accordance with increasing of solar diffuse pointing angle error. Also, it is found that RMSE increases in accordance with decreasing of wavelength. RMSE of estimation error for real part of refractive index is much greater than that for imaginary part of refractive index obviously.

(a) Real part

(b) Imaginary part

(c) Junge parameter
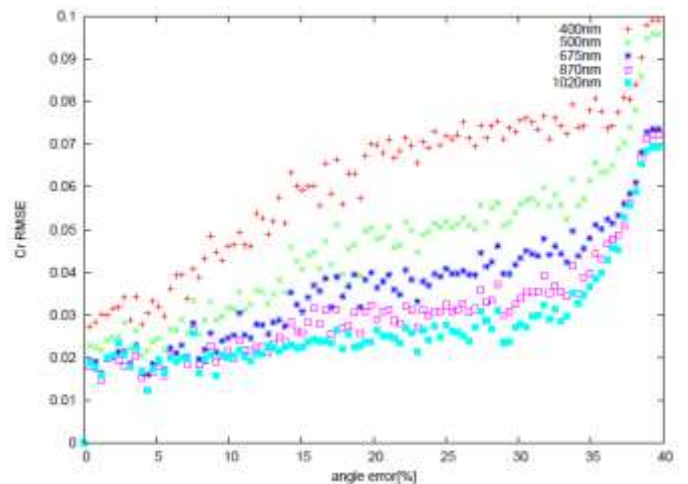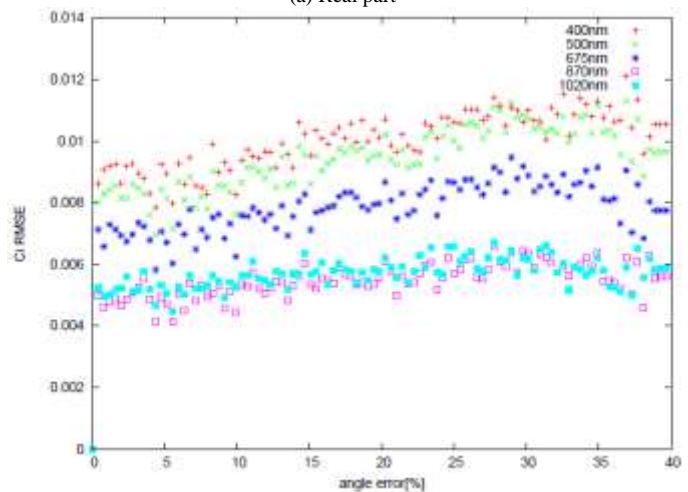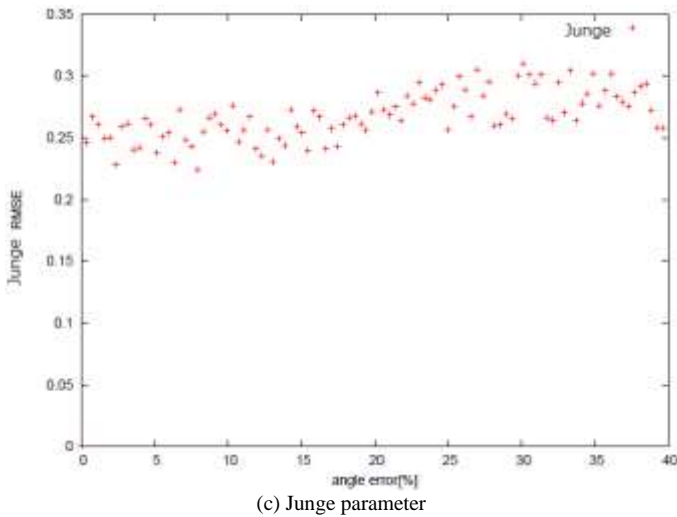
Fig. 5. RMSE of the aerosol parameter estimation caused by solar direct pointing angle errors

Also, solar diffuse pointing angle error dependency on real part of refractive index is much smooth in comparison to that on imaginary part of refractive index. In other word, the estimated imaginary part of refractive index is much diverse than the estimated real part of refractive index.

(a) Real part

(b) Imaginary part

(c) Junge parameter
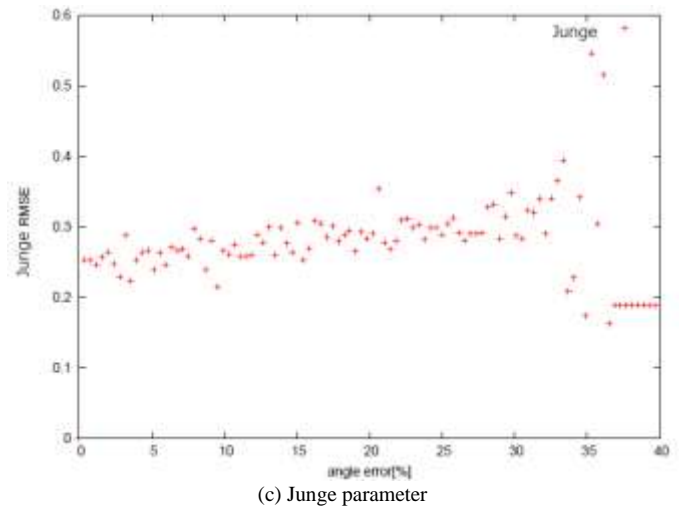
Fig. 6. RMSE of the aerosol parameter estimation caused by solar diffuse pointing angle errors

This is because of the actual real part of refractive index is much greater than that of imaginary part of refractive index. Furthermore, it is found that RMSE of Junge parameter increases with increasing of solar direct pointing error as shown in Fig.6.

IV. CONCLUSION

Estimation method of aerosol parameter by means of solar direct and diffuse irradiance measurements with the proposed instrument of fiber-ball radiometer without sun tracking mechanics is proposed. Sky-radiometer and aureole-meter is well known instrument which allows measurements of solar direct and diffuse irradiance for estimation of aerosol parameter.

The proposed fiber-ball radiometer also allows solar direct and diffuse irradiance measurements and is comparatively light as well as is composed without any mechanics so that it is portable and is enable to bring anywhere you want including test sites for field campaigns. Meanwhile, it is not always that the fiber-ball instrument points to the sun due to the error of the sun ephemeris calculations as well as sun track do not match to the actual one.

Influence due to pointing error on aerosol parameter estimation error is clarified. Possible maximum pointing error may cause some error on aerosol parameter estimation. Experimental results show that 0.43%, 42.23%, 2.12% root mean square errors are suspected for real and imaginary part of refractive index and Junge parameter as of 1.747, 0.0056 and 3.0 of typical case of atmosphere.

REFERENCES

[1] Shaw, G.E., Error analysis of multi-wavelength sunphotometry. Pure Appl. Geophys., 114, 1, 1976.

[2] Hoppel, W. A., J. W. Fitzgerald, G. M. Frick, R. E. Larson, and E. J. Mack, Aerosol size distributions and optical properties found in the

marine boundary layer over the Atlantic Ocean, J. Geophys. Res., 95, 3659-3686, 1990.

[3] Holben, B. N., et al., AERONET- A federated instrument network and data achieve for aerosol characterization, Remote Sens., 12, 1147-1163, 1991.

[4] Holben, B.N., and Coauthors, AERONET-A federated instrument network and data archive for aerosol characterization. Remote Sens. Environ., 66, 1-16. 1998.

[5] Aoki, K., T. Takamura, and T. Nakajima, Aerosol optical properties measured by SKYNET sky radiometer validation network. Proc. of the 2nd EarthCARE Workshop, 133-134, 2005.

[6] Redemann, R. P. Turco, K. N. Liou, P. B. Russell, R. W. Bergstrom, B. Schmid, J. M. Livingston, P. V. Hobbs, W. S. Hartley, S. Ismail, R. A Ferrare, E. V. Browell, Retrieving the vertical structure of the effective aerosol complex index of refraction from a combination of aerosol in situ and remote sensing measurements during TARFOX, J. Geophys. Res., 105, D8, 9949–9970, 2000.

[7] M.L.Clapp, and R.E.Miller, Complex Refractive Indices of Crystalline Hydrazine from Aerosol Extinction Spectra, Icarus, 23, 2, 396-403(8), 1996.

[8] R. Eiden, Determination of the complex index of refraction of spherical aerosol particles, Appl. Opt. 10, 749-757, 1971.

[9] G. E. Thomas, S. F. Bass, R. G. Grainger, and A. Lambert, Retrieval of aerosol refractive index from extinction spectra with a damped harmonic-oscillator band model, Appl. Opt. 44, 1332-1341, 2005.

[10] Kohei Arai, Aerosol refractive index retrievals with atmospheric polarization measuring data, Proceedings of the SPIE, 7461-06, 1-9, 2009

[11] Teruyuki Nakajima, et al., Use of sky brightness measurements from ground for remote sensing of particulate polydispersions, Applied Optics, Vol.35 No..15 pp.2672-2686 May 1996.

[12] Teruyuki Nakajima, et al., Retrieval of the optical properties of aerosols from aureole and extinction data, Applied Optics, Vol.22 No..19 pp.2951-2959 October 1983.

[13] M. A. Box and A. Deepak, An Approximation to Multiple Scattering in the Earth's Atmo-sphere:Almucanter Radiance Formulation, J. Atmos. Sci. Vol38 pp.1037-1048 1981.

[14] Mitsugu Toriumi, Hideaki Takenaka, Tadashi Kato, Toshikazu Hasegawa, Takashi Nakajima, Tamio Takamura and Teruyuki Nakajima: Estimation of Aerosol Optical Thickness by PAR Radiometer, Journal of The Remote Sensing Society of Japan, 30, 2, pp.81-89, 2010 .

[15] Tsutomu Takashima, Kazuhiko Masuda, Kohei Arai, Satoshi Tsuchida, Observation of Optical Property of the Atmosphere in Particular Aerosols at Deserted Areas In USA Using Sun-photometer and Polarization Spectrometer, Journal of Remote Sensing Society of Japan, Vol.20, No.3, pp.47-60, (2000).

[16] Kohei Arai, Influence of Non-Spherical Sea Salt Aerosol Particles Containing Bubbles on the Top of the Atmosphere Radiance, Journal of Remote Sensing Society of Japan, Vol.20, No.5, pp.32-39, (2001).

[17] Kohei Arai, Tatsuya Kawaguchi, Adjucency Effect of Layered Clouds taking Into Account Phase Function of Cloud Particles and Multi-Layered Plane Parallel Atmosphere Based on Monte Carlo Method, Journal of Japan Society of Photogrammetry and Remote Sensing, Vol.40, No.6, 2001.

[18] Kohei Arai, Yoko Takamatsu, Influence of Spume Aerosol Particles on the Top of the Atmosphere Radiance, Journal of Remote Sensing Society of Japan, Vol.23, No.4, pp.355-363, 2003.

[19] Kohei Arai, Xing Ming Liang, Estimation of Method for the Top of the Atmosphere Radiance Taking Into Account Polarized Up-welling and Down-welling Radiance, Journal of Japan Society of Photogrammetry and Remote Sensing, 44,3, 4-12,(2005)

[20] K.Arai, Monte Carlo simulation of polarized atmospheric irradiance for determination of refractive index of aerosols, International Journal of Research and Review on Computer Science, 3, 4, 1744-1748, 2012.

[21] K.Arai, Monte Carlo ray tracing based sensitivity analysis of the atmospheric and oceanic parameters on the top of the atmosphere radiance, International Journal of Advanced Computer Science and Applications, 3, 12, 7-13, 2012.

[22] K.Arai, Monte Carlo ray tracing based sensitivity analysis of the atmospheric and oceanic parameters on the top of the atmosphere radiance, International Journal of Advanced Computer Science and Applications, 3, 12, 7-13, 2012.

[23] Kohei Arai, Method for estimation of aerosol parameters based on ground based atmospheric polarization irradiance measurements, International Journal of Advanced Computer Science and Applications, 4, 2, 226-233, 2013.

[24] Kohei Arai, Sensitivity analysis and validation of refractive index estimation method with ground based atmospheric polarized radiance measurement data, International Journal of Advanced Computer Science and Applications, 4, 3, 1-6, 2013.

[25] Kohei Arai, Sensitivity analysis for aerosol refractive index and size distribution estimation methods based on polarized atmospheric irradiance measurements, International Journal of Advanced Research in Artificial Intelligence, 3, 1, 16-23, 2014.

[26] K.Arai, Vicarious calibration data screening method based on variance of surface reflectance and atmospheric optical depth together with cross calibration, International Journal of Advanced Research on Artificial Intelligence, 4, 11, 1-8, 2015.

[27] K.Arai, Kenta Azuma, Method for surface reflectance estimation with MODIS by means of bi-section between MODIS and estimated radiance as well as atmospheric correction with sky-radiometer, International Journal of Advanced Research on Artificial Intelligence, 4, 11, 8-15, 2015.

AUTHORS PROFILE

Kohei Arai, He received BS, MS and PhD degrees in 1972, 1974 and 1982, respectively. He was with The Institute for Industrial Science and Technology of the University of Tokyo from April 1974 to December 1978 and also was with National Space Development Agency of Japan from January, 1979 to March, 1990. During from 1985 to 1987, he was with Canada Centre for Remote Sensing as a Post-Doctoral Fellow of National Science and Engineering Research Council of Canada. He moved to Saga University as a Professor in Department of Information Science on April 1990. He was a counselor for the Aeronautics and Space related to the Technology Committee of the Ministry of Science and Technology during from 1998 to 2000. He was a councilor of Saga University for 2002 and 2003. He also was an executive councilor for the Remote Sensing Society of Japan for 2003 to 2005. He is an Adjunct Professor of University of Arizona, USA since 1998. He also is Vice Chairman of the Commission-A of ICSU/COSPAR since 2008. He received Science and Engineering Award of the year 2014 from the minister of the ministry of Science Education of Japan and also received the Bset Paper Award of the year 2012 of IJACSA from Science and Information Organization: SAI. In 2016, he also received Vikram Sarabhai Medal of ICSU/COSPAR and also received 20 awards. He wrote 34 books and published 520 journal papers. He is Editor-in-Chief of International Journal of Advanced Computer Science and Applications as well as International Journal of Intelligent Systsems and Applications. http://teagis.ip.is.saga-u.ac.jp/

Method for NIR Reflectance Estimation with Visible Camera Data based on Regression for NDVI Estimation and its Application for Insect Damage Detection of Rice Paddy Fields

Kohei Arai [1]
Graduate School of Science and Engineering
Saga University
Saga City, Japan

Osamu Shigetomi [2]
Saga Prefectural Agricultural Research Institute
Saga Prefectural Government,
Saga City, Japan

Kenji Gondoh [2]
Saga Prefectural Agricultural Research Institute
Saga Prefectural Government,
Saga City, Japan

Yuko Miura [2]
Saga Prefectural Agricultural Research Institute
Saga Prefectural Government,
Saga City, Japan

Abstract—**Method for Near Infrared: NIR reflectance estimation with visible camera data based on regression for Normalized Vegetation Index: NDVI estimation is proposed together with its application for insect damage detection of rice paddy fields. Through experiments at rice paddy fields which is situated at Saga Prefectural Agriculture Research Institute SPARI in Saga city, Kyushu, Japan, it is found that there is high correlation between NIR reflectance and Green color reflectance. Therefore, it is possible to estimate NIR reflectance with visible camera data which results in possibility of estimation of NDVI with drone mounted visible camera data. As is well known that the protein content in rice crops is highly correlated with NIR intensity, or reflectance of rice leaves, it is possible to estimate rice crop quality with drone based visible camera data.**

Keywords—*Rice crop; Rice leaf; Nitrogen content; Protein content; NIR reflectance; Water content; Size of rice leaves; Weight of rice crops*

I. INTRODUCTION

Vitality monitoring of vegetation is attempted with photographic cameras [1]. Grow rate monitoring is also attempted with spectral reflectance measurements [2]. Bi-Directional Reflectance Distribution Function: BRDF is related to the grow rate for tealeaves [3]. Using such relation, sensor network system with visible and near infrared cameras is proposed [4]. It is applicable to estimate nitrogen content and fiber content in the tealeaves in concern [5]. Therefore, damage grade can be estimated with the proposed system for rice paddy fields [6]. This method is validated with Monte Carlo simulation [7]. Also Fractal model is applied to representation of shapes of tealeaves [8]. Thus the tealeaves can be asse3ssed with parameters of the fractal model. Vitality of tea trees are assessed with visible and near infrared camera data [9]. Rice paddy field monitoring with radio-control drone mounting visible and Near Infrared: NIR camera is proposed [10] while the method for rice quality evaluation through

nitrogen content in rice leaves is also proposed [11].

The fact that protein content in rice crops is highly correlated with NDVI which is acquired with visible and Near Infrared: NIR camera mounted on drone is well reported [10]. It also is reported that nitrogen content in rice leaves is correlated to NDVI as well. Protein content in rice crop is negatively proportional to rice taste. Therefore, rice crop quality can be evaluated through NDVI observation of rice paddy field. Relation among nitrogen content in rice leaves, amount of fertilizer, NDVI and protein content in rice crops has to be clarified [11]. There are some indexes which show quality of rice crops, protein content, nitrogen content, etc. in the rice leaves. Meanwhile, there are some indexes for harvest amount, the number of ear in the stump, ear length, crop weight, etc. It should be depending on circumstances of geometric condition, soil condition, meteorological condition, water supply condition, fertilizer amount and rice stump density. Intensive study paddy fields have a variety of conditions. Drone mounted NIR camera has a good enough spatial resolution. Therefore, rice crop quality and harvest amount is evaluated as a function of water supply condition and fertilizer amount and rice stump density. These evaluation methods are well reported in the previous papers [12]. Another great concern is insect damages. Rice paddy fields situated in Asia are used to be damaged by insects, such as disappearing. In particular, brown colored disappearing are comes first depending on meteorological conditions followed by back black disappearing for the rice paddy fields in Japan. They are migrating from South-East Asian countries. They propagate so rapidly. Therefore, insect damages have to be detected so quickly and urgently. One of the effective methods for detection of insect damage is to monitor rice paddy field with drone mounted cameras. Un fortunately, most of cameras which can be mounted on drones are visible cameras. On the other hand, Normalized Difference Vegetation Index: NDVI is

quite useful for monitoring vigor, rice crop quality and harvest amount. It, however, can be calculated with Near Infrared: NIR data. Meanwhile, vigor, rice crop quality, and harvest amount are closely related to not only NIR reflectance but also green color reflectance, the sensitivity for the green color reflectance is poorer than that of NIR reflectance remarkably though. The proposed method is intended for estimation of NIR reflectance with visible camera data for estimation of NDVI which results in estimation of vigor, rice crop quality, and harvest amount.

The proposed method is described in the next section followed by experiments. The experimental results are validated in the following section followed by conclusion with some discussions.

II.   PROPOSED METHOD

The proposed method is based on linear regression. NIR camera data is compared to the visible camera data. The correlation coefficient between NIR intensity and Red, Green, Blue: RGB of visible intensity, and determination coefficients are estimated together with regressive equation.

III.   EXPERIMENTS

A. Rice Crop Field at Saga Prefectural Agriculture Research Institute: SPARI

Fig.1 (a) shows the Location (A) and (B) Layout of the test site of rice crop field at SPARI which is situated at 33°13'11.5" North, 130°18'39.6"East, and the elevation of 52 feet on the Google map. B and A in the Fig.1 (b) shows layout map for intensive study rice paddy fields.

Three are some experimental fields in the SPARI. Black rectangle in Fig.1 (b) indicates intensive study paddy field.
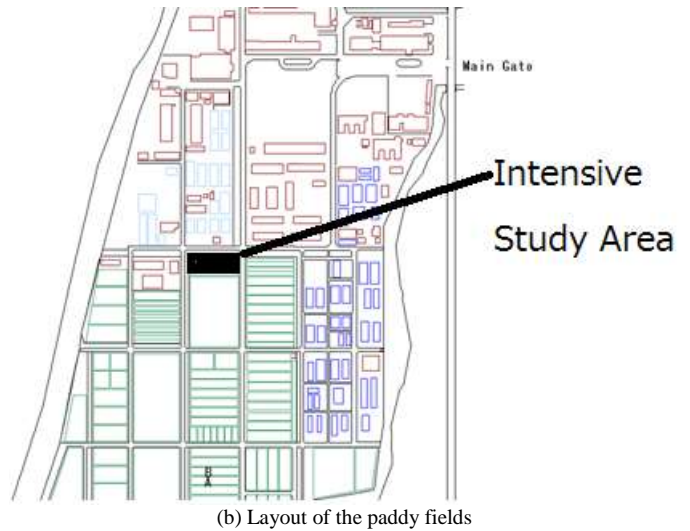
(b) Layout of the paddy fields

Fig. 1.   Location of Saga Prefectural Agriculture Research Institute: SPARI on Google map

"Sagabiyori" of rice specie and some others are planted in the intensive study area. In particular, no parricide is used in this field. Therefore, the field is damaged by insect when some insects come flying over the field easily.

B. Acquired Data

Drone mounted visible camera data are acquired at 9:00 on August 23, 13:00 on September 5, 9:00 on September 14, 14:00 on September 15, and 10:00 on September 16, while ground truth data and NIR reflectance are measured at 9:00-10:00 on August 23, and 10:00 on September 17, respectively. Fig.2 shows the acquired drone mounted camera images.

(a) Google Map
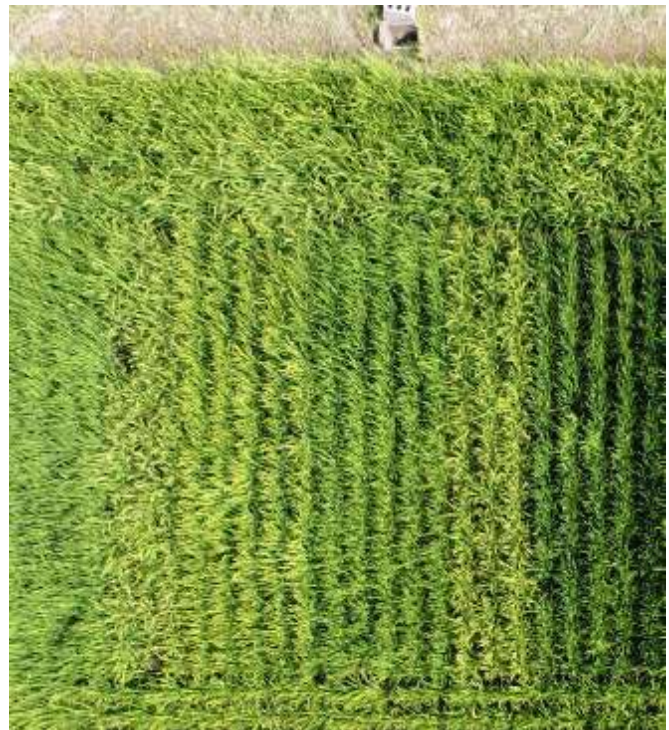
(a) 9:00 on August 23

(b)13:00 on September 5

(d)14:00 on September 15

(c) 9:00 on September 14

(e)10:00 on September 16

Fig. 2.   Acquired drone mounted visible camera data

Weather conditions are as follows,

August 23
1005.2 hPa
30.8 Deg.C
61.7 %
2.5 m/s
33:12'59.2"N, 130:18'45.6"E
GM:31.8-40.7

September 17
33:13'18.6"N, 130:18'40.6"E
30.7 Deg.C
66.4 %
1011.6 hPa
GM=7.7-22.6

GM denotes Green Meter value. Due to the fact that the GM value measured on September 17 is poorer than that on August 23, it is found that rice paddy field has severe damage due to insects.

These are a portion of drone mounted visible camera images at almost same area. Whole image color varies depending on the sun illumination angles. Also, two major damaged areas are getting expanded. In particular, large change can be seen during from September 5 and September 14. Meanwhile, ground based visible camera data and NIR camera data are acquired at 9:00-10:00 on August 23 and at 10:00 on September 17, respectively. Fig.3 shows the acquired visible and NIR camera imagery data. The field can be divided into two areas, damaged area and normal area clearly.

(b) Close-up visible image

(c) NIR image from far

(a) Visible image from far

(d) Close-up NIR image

Fig. 3.   Acquired visible and NIR camera imagery data.

Spectral reflectance is measured at the intensive study paddy fields on August 23 and September 17 2016. In the intensive study area can be divided into two portions, (1) damaged and (2) normal fields. (1) field is damaged due to insects while (2) field is not. These are under totally equal condition the species of rice crops are different from each other. These are named as "damage" and "normal" fields. The spectral reflectance measured on August 23 is shown in Fig.4 (a) while that on September 17 is shown in Fig.4 (b), respectively.

(a) August 23

(b) September 17
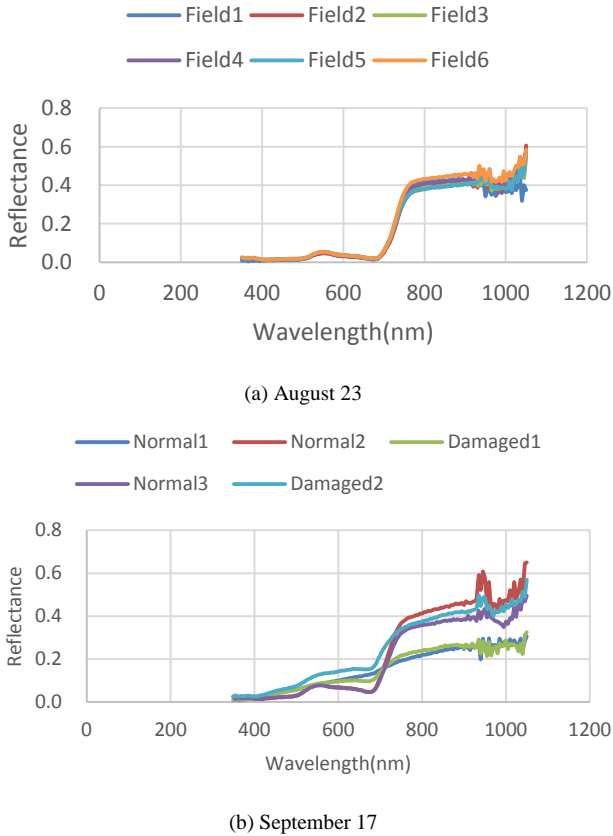
Fig. 4. Spectral reflectance measured at the intensive study paddy field in SPARI in 2016

It is clear that damaged paddy fields show remarkable low reflectance at the near infrared wavelength region while that for normal paddy fields show stable NIR reflectance in comparison to that of August 23.

C. Regressive Analysis

From the drone based visible camera data, insect damage trend can be analyzed. NIR and RGB intensities are plotted as a function of time being as shown in Fig.5. The detailed color and NIR intensity is shown in Table 1 as well. In these figure and table, suffix d denotes "damaged area" while n denotes "normal area", respectively.

The color of the damaged area is changed to white. Therefore, intensity is increased after the rice paddy field is damaged due to insects.
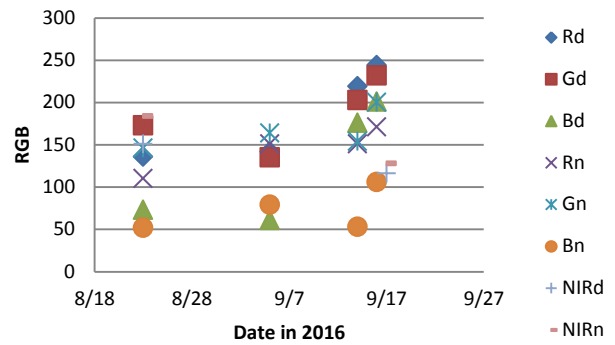
Fig. 5. RGB color intensity trend

TABLE I. DETAILED COLOR INTENSITY TREND

VIS	Rd	Gd	Bd	Rn	Gn	Bn
8/23	136	173	73	110	146	52
9/5	142	135	61	151	164	79
9/14	219	203	176	151	154	53
9/16	244	232	201	171	200	106
NIR	Rd	Gd	Bd	Rn	Gn	Bn
8/23	235	108	151	249	115	184
9/17	243	103	116	199	77	128

On the other hand, color intensity of the normal rice paddy field is stable, relatively. Also, it is found that green color intensity has almost same tendency as NIR intensity tendency. Therefore, there is a possibility of estimation of NIR reflectance with green color intensity.

Fig. 6 and Table 2 shows the results from the regressive analysis between RGB and NIR reflectance measured on August 23 and September 17 2016. The determination coefficient is more than 0.94 for the correlation between Green reflectance and NIR reflectance as shown in Fig.6. Therefore, it can be concluded that it is possible to estimate NIR reflectance with green color reflectance. In other word, it is possible to estimate NDVI by using drone mounted visible camera data.
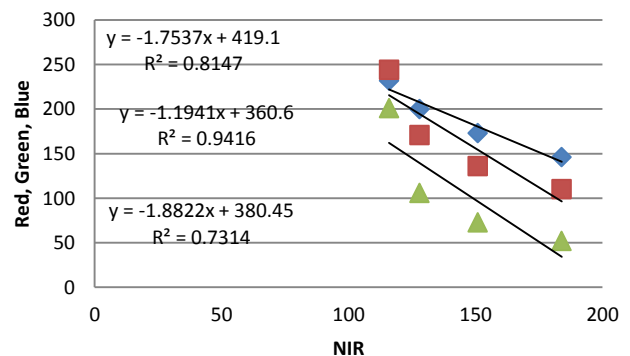
Fig. 6. Results from the regressive analysis

TABLE II.   RELATION BETWEEN NIR INTENSITY AND RGB INTENSITIES

NIR	R	G	B
116	244	232	201
128	171	200	106
151	136	173	73
184	110	146	52

IV.   CONCLUSION

Method for Near Infrared: NIR reflectance estimation with visible camera data based on regression for Normalized Vegetation Index: NDVI estimation is proposed together with its application for insect damage detection of rice paddy fields. Through experiments at rice paddy fields which is situated at Saga Prefectural Agriculture Research Institute SPARI in Saga city, Kyushu, Japan, it is found that there is high correlation between NIR reflectance and Green color reflectance. Therefore, it is possible to estimate NIR reflectance with visible camera data which results in possibility of estimation of NDVI with drone mounted visible camera data. As is well known that the protein content in rice crops is highly correlated with NIR intensity, or reflectance of rice leaves, it is possible to estimate rice crop quality with drone based visible camera data.

It can be concluded that it is possible to estimate NIR reflectance with green color reflectance. In other word, it is possible to estimate NDVI by using drone mounted visible camera data.

ACKNOWLEDGEMENT

REFERENCES

[1] Wiegand, C., Shibayama , M, Yamagata , Y, Akiyama, T., 1989. Spectral Observations for Estimating the Growth and Yield of Rice, Journal of Crop Science, 58, 4, 673-683, 1989.

[2] Kohei Arai, Method for estimation of grow index of tealeaves based on Bi-Directional reflectance function:BRDF measurements with ground based netwrok cameras, International Journal of Applied Science, 2, 2, 52-62, 2011.

[3] Kohei Arai, Wireless sensor network for tea estate monitoring in complementarily usage with Earth observation satellite imagery data based on Geographic Information System(GIS), International Journal of Ubiquitous Computing, 1, 2, 12-21, 2011.

[4] Kohei Arai, Method for estimation of total nitrogen and fiber contents in tealeaves with grond based network cameras, International Journal of Applied Science, 2, 2, 21-30, 2011.

[5] Kohei Arai, Method for estimation of damage grade and damaged paddy field areas sue to salt containing sea breeze with typhoon using remote sensing imagery data, International Journal of Applied Science,2,3,84-92, 2011.

[6] Kohei Arai, Monte Carlo ray tracing simulation for bi-directional reflectance distribution function and grow index of tealeaves estimation, International Journal of Research and Reviews on Computer Science, 2, 6, 1313-1318, 2011.

[7] Kohei.Arai, Fractal model based tea tree and tealeaves model for estimation of well opened tealeaf ratio which is useful to determine tealeaf harvesting timing, International Journal of Research and Review on Computer Science, 3, 3, 1628-1632, 2012.

[8] Kohei.Arai, H.Miyazaki, M.Akaishi, Determination of harvesting timing of tealeaves with visible and near infrared cameradata and its application to tea tree vitality assessment, Journal of Japanese Society of Photogrammetry and Remote Sensing, 51, 1, 38-45, 2012

[9] Kohei Arai, Osamu Shigetomi, Yuko Miura, Hideaki Munemoto, Rice crop field monitoring system with radio controlled drone based near infrared cameras through nitrogen content estimation and its distribution monitoring, International Journal of Advanced Research in Artificial Intelligence, 2, 3, 26-37, 2013.

[10] Kohei Arai, Masanori Sakashita, Osamu Shigetomi, Yuko Miura, Estimation of Protein Content in Rice Crop and Nitrogen Content in Rice Leaves Through Regression Analysis with NDVI Derived from Camera Mounted Radio-Control Drone, International Journal of Advanced Research in Artificial Intelligence, 3, 3, 13-19, 2013

[11] Kohei Arai, Masanori Sakashita, Osamu Shigetomi, Yuko Miura, Estimation of Protein Content in Rice Crop and Nitrogen Content in Rice Leaves Through Regression Analysis with NDVI Derived from Camera Mounted Radio-Control Drone, International Journal of Advanced Research in Artificial Intelligence, 3, 3, 13-19, 2013

AUTHORS PROFILE

Kohei Arai, He received BS, MS and PhD degrees in 1972, 1974 and 1982, respectively. He was with The Institute for Industrial Science and Technology of the University of Tokyo from April 1974 to December 1978 and also was with National Space Development Agency of Japan from January, 1979 to March, 1990. During from 1985 to 1987, he was with Canada Centre for Remote Sensing as a Post-Doctoral Fellow of National Science and Engineering Research Council of Canada. He moved to Saga University as a Professor in Department of Information Science on April 1990. He was a counselor for the Aeronautics and Space related to the Technology Committee of the Ministry of Science and Technology during from 1998 to 2000. He was a councilor of Saga University for 2002 and 2003. He also was an executive councilor for the Remote Sensing Society of Japan for 2003 to 2005. He is an Adjunct Professor of University of Arizona, USA since 1998. He also is Vice Chairman of the Commission-A of ICSU/COSPAR since 2008. He received Science and Engineering Award of the year 2014 from the minister of the ministry of Science Education of Japan and also received the Bset Paper Award of the year 2012 of IJACSA from Science and Information Organization: SAI. In 2016, he also received Vikram Sarabhai Medal of ICSU/COSPAR and also received 20 awards. He wrote 34 books and published 520 journal papers. He is Editor-in-Chief of International Journal of Advanced Computer Science and Applications as well as International Journal of Intelligent Systsems and Applications. http://teagis.ip.is.saga-u.ac.jp/

Contribution to Securing Connections in a Communications Network: Modeling and Conception of a Fraud Detector

Souad EZZBADY

Dept. of Mathematics and Computer Science
Faculty of Sciences Ben M'sik
Hassan II University Mohammedia, Casablanca, Morocco

Abdelwahed NAMIR

Dept. of Mathematics and Computer Science, Faculty of
Sciences Ben M'sik
Hassan2 University - Mohammedia, Casablanca, Morocco

Abstract—**With the explosion in the volume of data, it became primordial for businesses and responsible to implement new tools to detect in real time the unusual changes in its communications network to address all security holes. In this sense, one of the most recently used solutions is the migration of relational databases to the directed graph databases, thanks to his capacity to manage huge and complex bases, and his easiness of management of security. It is in this sense that this work is located, whose objective is firstly to model the data as a graph with nodes representing users and arcs represent the connection between users. And secondly to monitor connections of links between the different nodes to facilitate the task to one who will handle this data with the ultimate goal of detecting cases of fraud. Indeed, it is to propose a modeling and conception of a technique to improve the communication network management to monitor and report real-time alerts in the event of fraud.**

Keywords—Directed graph database; strongly connected components; Security Management; Theorem graph; communication network

I. INTRODUCTION

The databases are increasing day by day in all areas. So to present such a large volume of data, we must find a useful method that will facilitate access to information securely, at any time and will represent the users and the links between them [1], [8].

Moreover, it is increasingly difficult today to secure the information correlated data collected. Therefore, we must find a way to solve this problem.

At this fact, numerous studies and developments have proposed solutions such as graph database with its strengths, its issues and challenges. These bases are provided for storing and processing of highly connected data, easily manage a complex and highly interdependent network of users and transactions [1].

To benefit from effective security of data, companies need a protective layer bonded to the data, to identify, prioritize and optimize risk. From where the need to develop new tools to help detect real-time changes to make the best decisions [6], [7].

We suggest in this paper a method to improve

management and communication network security, proposing a conception of a technique used to demonstrate this approach. That said, network monitoring, and is another entity security and essential to achieve complete protection. To do this, first we model the communication network (eg a company) by a directed and connected graph. Second, it turns this graph in its reduced graph to identify connections to monitor and instantly control. Thirdly we focus on the field of access (read and write within the company) and detect, in real time, all that adds or removes or accesses a maliciously.

The result of this work consists of three sections: in the first paragraph, it addresses the problem being treated. In the second paragraph, it gives a solution to the problem and in the latter; it is proposed a conception computerized fraud detection. The conclusion shows the outline of the study and of our contribution and also provides various extensions and possible future works.

II. ISSUES AND PROBLEMATIC ADDRESSED

A security database has become increasingly a paramount need, before the large volume and complex data. Especially security threats are becoming more frequent and dramatic. So the information system seeks to protect the actions of hackers looking to surpass the protections put in place.

Take the example of a communications network made up of several departments:

- IT department

- HR Department

- Administrative department

- The exterior ...

Each department has access to separate directories, for example the HR department to files concerning the salaries of employees who are confidential and access a collaborator in this matter is considered FRAUD. But when users have access privileges to a database that exceeds the requirements of their job function, they can abuse these privileges for malicious purposes. Therefore, the objective of our research is to perform modeling and technical design to detect in real time any changes in the database whatsoever modified from the

application or directly from the comics.

We model the data as a graph consisting of nodes and relationships, for displaying the access rights of each user with its corresponding files. If a third party has added a direct access to the database without using the application, it is considered fraud and illegal and the app will generate a signal indicating the properties of the added relationship in an illegal manner.

This issue of fraud or attack resulting changes in two levels of programs is:

The fraudulent character changes

- To assign the benefits of the program, according to the purpose of fraud.

Example: transfer money to another account.

Sabotage character changes

- To destroy with varying motivations systems or data.

So the goal of our research is to fill this gap by facilitating the security of important data.

III.   THE PROPOSED MATHEMATICAL SOLUTION

To address the problem addressed, we modeled the data or information related to a user by a directed graph that maps all nodes with their corresponding relationships.

The basic function of the proposed solution is to keep an eye on the graph, and report a warning if there is a fraud.

Later we will see two parts:

- The modeling part: aims to model the data as a graph and recall the points which will be needed to construct the reduced graph.

- The application part: it is explained in this part of the various components of the application.

A. Mathematical modeling

We modeled these data as a graph, where the user will be represented by a node, and the relationship between the nodes will be materialized by a directed arc from node A to node B, that is to say, users A and B and the connection from A to B. Then we translated this graph in its reduced graph to optimize the connections to monitor.

We will present a number of concepts that will be needed in the next chapters. For this one begins with a reminder on graph theory, strongly connected components, reduced graph...[2],[3],[4],[5].

B. Communication network

1) Directed Graph

- A directed graph G is a relation on a finite set X, denoted G = (X, U). X is the set of vertices or nodes (representing in this case the users) and U consists of all couples $(x, y) \in X \times X$ which are related, it is called the set of arcs (representing in this case the connections); [2], [3], [4], [5].

- A path G width $p \epsilon N^*$ of a vertex x to a vertex y is a sequence of vertices; $(x_1, x_2, ... x_p)$ such as $x = x_0, y = x_p$ and $(x_{i-1}, x_i) \in U$ for i = 1,2, ..., p. x is the original and there is the end of the path (the orientation is followed); [2], [3], [4], [5].

- A chain of G the length $p \epsilon N^*$ a vertex x to a vertex y is a sequence of such summits $(x_1, x_2, ... x_p)$ such as $x = x_0, y = x_p$ and $(x_{i-1}, x_i) \in U$ or $(x_i, x_{i-1}) \in U i = 1,2, ..., p$. x and y are the ends of the chain; [2], [3], [4], [5].

- G is said to be connected if for any pair $(x, y) \in X \times X$ with x≠y, there is a chain of x to y; [2],[3],[4],[5].

- G is called strongly connected if for all couples $(x, y) \in X \times X$ with x≠y, there is a path from x to y and another path from y to x. [2], [3], [4], [5].

- G A circuit is a path to a summit itself. [2], [3], [4], [5].

Note 1 : Numerically, G

- ✓ Connected, if there is a chain which passes through all the vertices;
- ✓ Strongly connected, if there is a circuit which passes through all the vertices.

- Called strongly connected component of G, any subset of X formed of top connected by the following relationship:

x R′y ⇔ there is a path x to y and another path from y to x.

Note 2: Family $\{C_i\}_{i=1}^k$ all strongly connected components of G form a partition of X, that is to say:

- ✓ $C_i \cap C_j = \emptyset$ par i ≠ j
- ✓ $U_{i=1}^{i=k} C_i = X$.

- A reduced graph of the graph G is the graph G' to which each node is associated with a strongly connected component of G. In addition, an arc connects a node x' to a node y' in the graph G' if there is an arc connecting x to y in G where x is in the strongly connected component of G associated with x 'and y belongs to the strongly connected component of G associated with y'.

Note 3: the vertices of the reduced graph are strongly connected components of G.

Example 1: Let the communications network modeled by
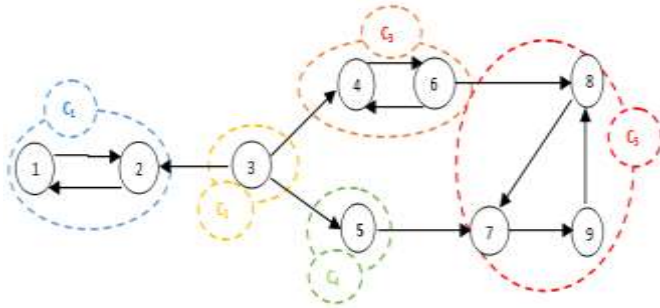
the given graph G:

Fig. 1.   Graph G

- G is connected because (1, 2, 3, 4, 6, 8, 9, 7, 5) is a chain that passes through all the vertices. But it is not strongly connected because there is no path from the node 2 to node 3.

- The strongly connected components are:

$C_1 = \{1,2\}$, $C_2 = \{3\}$, $C_3 = \{4, 6\}$, $C_4 = \{5\}$ and $C_5 = \{7, 8, 9\}$.
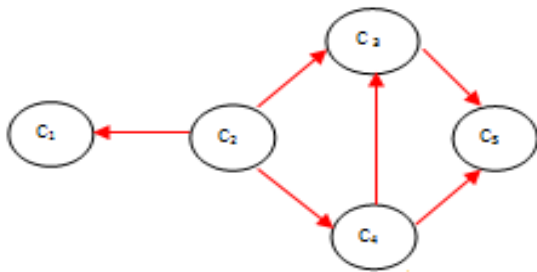
- It gets its reduced following graph:

Fig. 2.   Graph reduced G'

It adds another strongly connected component E which is external clients (all that is external to the company's communication network) and connected by an arc facing the strongly connected components of the graph reduces E. obtained the following graph:
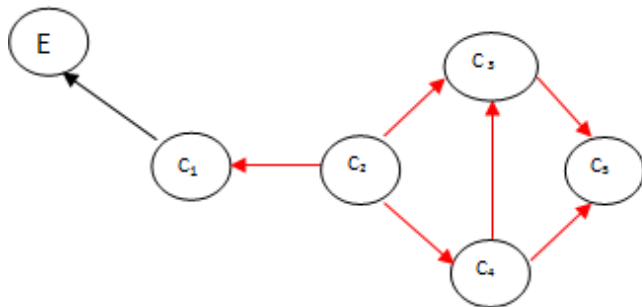

Fig. 3.   Graph reduced G' with external clients

C. *The important connections to control or monitor instantly*

Is a communication network, it can be modeled by a connected graph G whose nodes are the users and the arcs are connections.

- Arc called critical any arc between the strongly connected components of the reduced graph.

- Called non-critical arc any arc between the vertices of a strongly connected component.

Example 3: Example 1 arc (3.2) is critical, and the arc (8.7) is not critical.

Result:

There is Fraud, If there is an addition of an arc oriented in the opposite direction of a critical arc.

Can be mathematically modeled fraud in a communications network by a directed arc. This arc cannot beings within a strongly connected component because otherwise it would have no influence due this fraud cannot uncritical beings arc. So fraud is an arc oriented in the opposite direction of a critical arc.

In fact there are two types of addition of directed edges:

- In the addition of a modeled oriented arc in the strongly connected component in this case it has no influence.

- An addition of an arc oriented in the opposite direction of a critical arc, in this case there is a fraud, as in the graph G if there is an addition of an arc oriented summit a node 2 to the node 3 so it is considered fraud because the node 2 has no relay to reach the node 3.

IV.   CONCEPTION AND REALIZATION A DETECTOR

After the modeling of the communication network by a graph, one shows the different objectives of this conception:

- Facilitate access to databases of users who are connected when linked together in the graph via a simple user interface without the need for SQL scripts.

- Visualize, analyze and quickly correlate database activities from any angle via a simple user interface without the need for SQL scripts.

- Monitor and record all activities authorized and unauthorized access to sensitive data in real time.

- Detect vulnerabilities and fraud and leakage in real time databases.

- Report and block attacks to databases and unauthorized activities in real time. Whether original application or a privileged user on the network or locally on the server database,

So to answer all security aspects of a database server by providing real-time protection, we must control the various access.

These aspects include:

- Defining a security policy, preserve confidentiality,

- integrity

- Data availability.
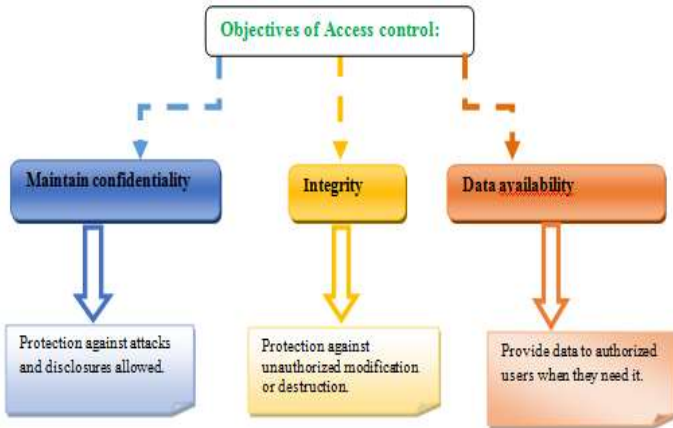
Fig. 4.   Access Control Objectives

D. Computerization of problem

In this paragraph, we will submit the application with the different components, explaining the role of each. Our application showing "Who, What, Where and How" each share between users.

This application has 3 parts:

- *User management*: This part aims to add, modify and delete users (that is to say that user will make use of this application).

- *Accordion users*: This part aims to add, modify and delete users. (Create the graph that is to say nodes and arcs)

- *Dashboard:* with all interconnected nodes (all given access rights).

- *List of actions*: Containing a list of actions or facts access via the application, if access is allowed nothing is reported, otherwise a warning will be triggered indicating the fraudulent act with the name of the affected user.

Fig. 5.   First window in the application

For more explanation we will give an example of the application:

- The following windows is reserved for users, it contains all the components of the application as the note:

- The interface reserved for single users only contains two parts. the first for file management and second for the dashboard:

Fig. 6.   Permission to access for users

Fig. 7.   First window with the components of the application
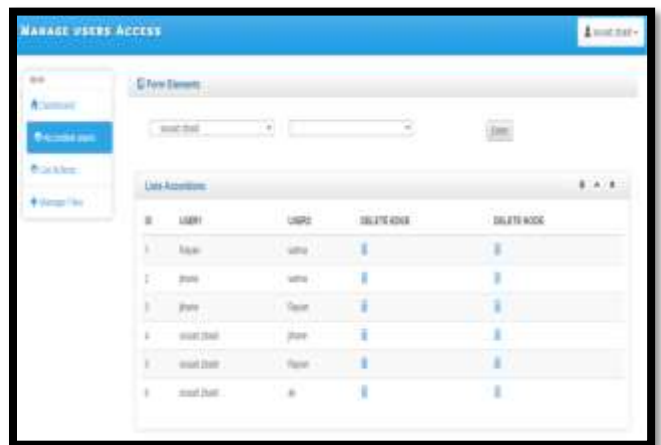
Fig. 8.   The Building of links between nodes

- We start with present the first part of the application, this windows and defines the different interconnections between the nodes:

- After defining the paths or links between different users or nodes (that is to say, user "Souad" in "Ali" user so on) is obtained:

- At the application level, we tried to achieve the following points:

  ➢ All nodes in the system visualize exactly the same data at the same time (data consistency).

  ➢ Loss or deletion of nodes does not prevent other nodes to continue to function properly, the data remains accessible (data availability).

  ➢ No less a total failure of the network failure may cause the system to respond properly.

If partitioning into sub-networks, each must operate autonomously.

- We get the following graph on which will monitor the links between the nodes and their reactions and a graph data structure, it is possible to find data in a very powerful way, browsing a graph, ie by navigating relationships. It is at this level that the graph takes all its power: find the shortest path between two nodes, find - from a given node - all nodes having a relationship "Rayan" for example.
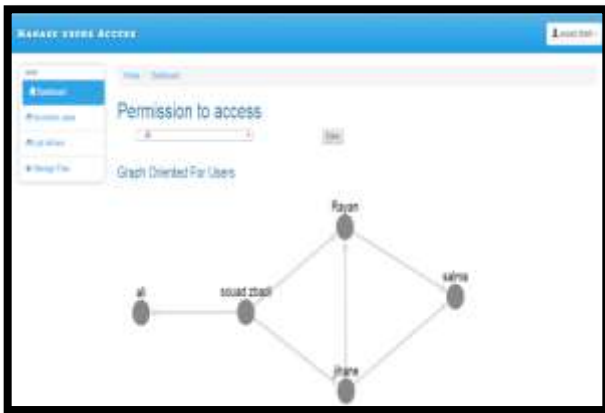
Fig. 9. The result of built graph

- In this interface is treated two cases:

  ✓ the first case: The "A" user is allowed to access the user "B".

Eg "Souad" user permission to access the user database "Rayan" as shown in the graph above.
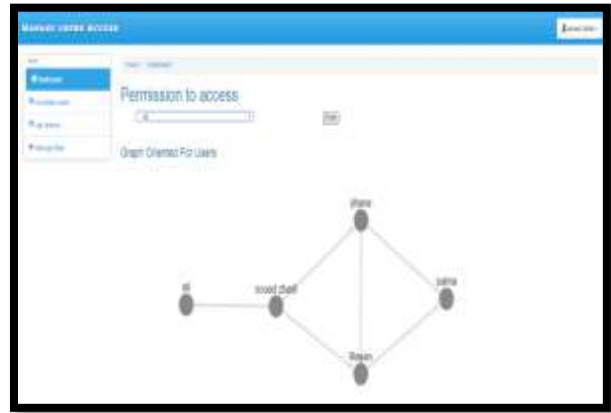
Fig. 10. Example for permission of user to access

So when is connected to the user database "Rayan" you can download the files you need:

Fig. 11. Access to the data

- The second case: If, for example "Souad" user has no right to access the user database "Salma" is at this level that our proposal acquires its importance. That is to say any connection to a database whose context does not match the defined information for which the user profile triggers an alert.

Previously, the user of a database can end up with excessive privileges for the simple reason that database administrators do not have the time to define or update the control mechanisms of the conditions of access for each user. Consequently, all users or large groups of users have the default set of access rights which far exceed the requirements of their specific function.
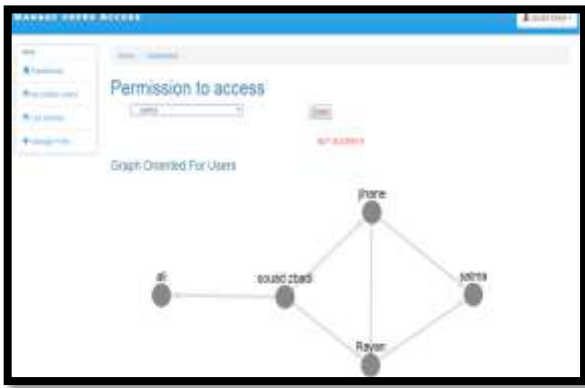
Fig. 12. Case of fraud

When unauthorized access is made via the application, an alert will be triggered indicating the name of the user who made the fraudulent act, and when exactly. This access control mechanism would allow the official (High placed malicious) University; described above; update students coordinates, but would trigger an alert if it tried to edit notes.

As shown in the following interface accordions users pane, which indicates that the user "Souad" attempted to access the database of "Salma" and what time, another highlight of this section is that the history of the list of actions is always archived, and no one can erase. So despite that "Souad" be responsible for the management of the application, if it commits fraud it will automatically added to the list in real time.

Fig. 13. History of all cases of fraud and cases of permission access

Throughout this document we presented the proposed solution to the problem on two levels: the theory and practice.

To demonstrate that in most cases, simply a relational database associated with a relational schema properly made to meet your needs.

But now whether to store enormous amounts of data (Peta bytes), with many users that generate high traffic, a distributed architecture is necessary. These data are extremely valuable and confidential require agencies to audit access to sensitive data and protect against attacks and malicious behavior.

V. CONCLUSION

As the threats and risks to databases and vital resources are becoming increasingly important, the implementation of controls is now essential. Given the increased risks, particularly the risk of fraud, it is essential to find effective solutions to block those who want to commit or conceal fraud and minimize the risk of loss that may arise from various types of threats.

In this sense is this work. Whose objective is to propose a design technique based on graphs, and whose ultimate goal is to secure the data and detect fraud. It opens the way to various research perspectives:

- Extend this work and write to the graph-oriented databases.

- Connect this application to large databases that is to say the Big Data

- Use Orient DB to develop this application.

References

[1] Odile PAPINI Part II Course 3 (continued): Security basesde data: ESILUniversité the Mediterranean Odile.Papini@esil.univ-mrs.fr

[2] J.A. Bondy, U.S.R. Murty, Graph Theory with Applications, North-Holland, New-York, (1976).

[3] C. Godsil, G. Royle, Algebraic Graph Theory, Graduate Text in Math. 207, Springer,(2001).

[4] Ministère de l'éducation nationale, Introduction d'éléments de la théorie des graphes, accompagnent de la mise en oeuvre des programmes, (2001).

[5] V. Chandola, A. Banerjee, et V. Kumar, Anomaly detection - a survey (Technical Report TR 07-017). Computer Science Department, University of Minnesota.

[6] V. Chandola, A. Banerjee, et V. Kumar, Anomaly detection - a survey. ACM Computing Surveys, 41, 2009.

[7] Y. Bejerano and R. Rastogi. Robust Monitoring of Link Delays and Faults in IP Networks. In Proceedings of IEEE Infocom, 2003.

[8] N. Biggs, Algebraic Graph Theory, 2nd Edition, Cambridge Math. Library, (1993).

[9] L. Page, S. Brin, R. Motwani, T.Winograd, The PageRank Citation Ranking: BringingOrder to the Web, Technical Report, Stanford University, 1998.

[10] J. Miles Prystowsky, L. Gill, Calculating Web Page Authority Using the PageRankAlgorithm,http://online.redwoods.cc.ca.us/instruct/darnold/LA PROJ/.

[11] S. P. Radziszowski, Small Ramsey Number, Dynamic surveys, The Electronic Journal of Combinatorics, http://www.combinatorics.org/Surveys/ds1.pdf

[12] O. Ore, Graphs and their uses, version r´evis´ee par R. J. Wilson, New Mathematical Library 34, Math. Association of America.

[13] R. Cabane, Th_eorie des graphes, Techniques de l'Ing_enieur, Trait_e Sciences fondamentales, document AF205.

Performance Analysis of Solar Photovoltaic Cells for Telecommunication Cellular Network in Remote Areas of Pakistan

Abdul Ghayur[1]
Department of Electrical Engineering
Iqra National University
Peshawar Pakistan

Sanaullah Ahmad[1]
Department of Electrical Engineering
Iqra National University
Peshawar Pakistan

Manzoor Ahmad[1]
Department of Electrical Engineering
Iqra National University
Peshawar Pakistan

Abstract—In this research design and implementation of solar photo voltaic cell is done for base transceiver system (BTS) of telecom cellular networks in remote areas of Pakistan, to accomplish this task investigation is done regarding the present alternate power source of base transceiver system (BTS) that is the generator sets used as a stand-by, prime and t-prime source. This research will examine that generator sets fuel consumption and maintenance cost is considerably high and the cellular company has to pay a lot to keep a site on air and to overcome the connectivity issues.To resolve these issues this research is aimed to implement solar technology on BTS, for this purpose exploration is done regarding BTS rectifier system and suggested to use power on distribution systems 16 (PODS 16), latest technology evolution (LTE) based instead of the simple BTS rectifier, this new rectifier is intelligent and has redundant ways to overcome power issues as it has the capability to work directly on solar panel equipments and it requires DC supply. Other important factor is that solar panel recharge batteries for power backup and to keep the site on air during night time. Different cost comparison of solar and generator sets have been done by taking real data of different remote areas sites and in the end it is concluded that solar is the alternate costless, environmental friendly source of energy for BTS and can be implemented both for off-grid and on-grid systems.

Keywords—*Network performance parameters, Power on distribution system, On-grid-Solar systems, Latest technology evolution*

I. INTRODUCTION

Power sector in Pakistan is using limited and indirect sources of energy,power load shedding in telecommunication companies has considerably affected network performances and a user faces problems of connectivity, to resolve these type of connectivity issues and to keep the site on air other renewable source of energy like solar is added to the BTS site, with the addition of Power on Distribution Systems (PODS16) rectifiers. Analysis on solar and its backup batteries is done in contrast with the diesel generators on the basis of cost and maintenance problems.Different data of the Mobilink cellular company about the work plan and daily activity report of the field engineer have been carefully examined by the author and analyzed. This data contains information about North2 regions of KPK in Pakistan that contain remote sites. Currently for power generation Genset are used on BTS sites. In remote sites of BTS stand-by, prime and t-prime gensets are installed that

supply power to the BTS. During non availability of utility power currently genset technology is used for running BTS system.In remote ares at least one BTS is installed in each cell which is hexagon shaped.these cells combines and form of a cluster.A cluster contains more than one BTS which is linked to a Hub site. When a Hub BTS goes down due to power issue the other linked BTS automatically goes down and the dis-connectivity issue of that area take place. This is a serious challenge for technical teams. Some of the issues due to non availability of power are given below.

- Connectivity
- Frequency reuse
- Network manageability problem
- Scalability
- Security
- Company loss and other trade offs associated with it

A. Research Significance

Telecommunication Companys competency is growing day by day. The telecommunication companies in Pakistan are looking to provide more and more services to their customers so that they can improve their market shares. So thats why they are searched for such type of operations with reduce in cost and quality of service in which they feel free and concentrate on their core business. In the current situation telecommunication companies in Pakistan are facing dis-connectivity issues in remote areas. Due to dis-connectivity issues company faces to a big loss.To avoid loss and facilitate users an alternate and direct source which is solar photo voltaic cell is an good option.

B. Research Contribution

In this research we have targeted Mobilink Company, Nokia Company Rectifiers and Solar Power One (SPO) company equipment as a case study.To examine better results we have collected data for Daily Fuel Cost, Daily Activity Report, List of Remote Sites for North-II Region from the targeted Comapnies.

The main contributions of this research are:

- To examine the expertise of Solar Power One company.

- To examine how this Solar Photo Voltaic system is best option for Off-grid and On-grid stations.

- To prove that solar is cost effective as compared to other energy sources.

- To analyze benefits of solar relating other power sources .

- To examine remote areas BTS sites of the mobilink company

- To note BTS locations and their power status like prime, t-prime and standby.

- To investigate the benchmark,average NOC hours and load shedding time.

- To investigate about those areas where network disconnectivity issues occurs frequently.

- To examine monthly and yearly cost of fuel and maintenance.

- To point out the different ratings of gensets.

II. Background

The energy that is produced by the sun rays is called solar energy.Hydrogen that has an approximate of 650000000 tons of elements is converted to Helium in seconds is the ultimate energy source from the sun, this conversion of hydrogen to helium is called as a thermonuclear process. Heat plus the electro magnetics radiations are formed during this process. Wind, Tidal, Biomass, and Hydel are the indirect incomes of the solar energy while sunlight rays that are the radiations are the direct sources of solar energy [1]. An approximate of 100000 tetra watts (TW) of solar energy reaches the earth in approximately one hour duration this much of energy is sufficient to meet the demands of the whole globe or world for one year time period it means 1hour of 100,000TW= 1 year supply of energy for the whole world [2]. Kim a scientist said that the total 1, 62, 000 (Tera watts) of Solar energy reaches the earth but due to some factors half of it stays in the atmosphere or distributes in the atmosphere and less than half strikes the earth surface or reaches the earth apparent body [3], so it means that about 0.5 (Tera watts) of energy from the sun that is the solar radiations are used by human beings [4]. [3] done a research and he realized that other sources of energy might discharge out if they are used in tremendous amounts like coal, gas and oil, whereas the direct source of energy like wind, water, sun are renewable sources and might not be limited as they are unlimited in contrast to coal, gas and oil that are limited [5], so there is a casual that these resources might not be available after a certain amount of time period [6] or these resources might run out due to its so much use.Most of the areas in our country are directly linked with solar radiations as sunlight or sun shines for about 2000-3500 hours per annum. A total of 2.0 to 3.1 Megawatts hour per meter square per year or MW h /m^2/$year$ that is equivalent to 6.7KW/h/m^2 day of the power [7] capability. Pakistan has an ultimate climate to take advantage of the solar radiations. Our province Baluchistan that has the largest square feet area

is measured to be area having the peak solar energy rays or radiations. Baluchistan province of Pakistan is supplemented with the maximum solar light radiations.20-21MJ/m^2/day [8] is the Baluchistan daily solar radiations figure, these values may vary slightly with little difference and are ideal for solar panels and solar appliances. The average sun shine in Pakistan is 8 to 9 hours [9] which is best for solar panels to give a good output.

III. Methodology

This research is composed of quantitative analysis which contain cost analysis for fuel consumption of gensets, cost analysis for replacing solar system, power calculation required for BTS, solar panel power generation and batteries play back period. Data was collected using face to face interviews and by questionnaires. the range of employees for data collection was upto 300 from all companies.

A. Population

Currently below mentioned company are working in Pakistan which are providing their services in the field of wired/wireless communication and broad bands.

Wired/wireless companies in Pakistan

- Mobilink

- PTCL

- Naya Tel

- World Call

- Telenor

- NTC

- Ufone

- Warid

- Zong

Companies in the field of equipment manufacturer and transporter.

- Power One

- Schneider

- Nokia rectifiers

B. Sample and Sample Size

The targeted company for our research is Mobilink and the region was North-II region. Due to easily accessibility of data and regional office of Mobilink company we kept it as a sample. Analysis on solar is achieved by the help of the staff of solar company private limited, and the key points of analysis include.

- Finding the load of Solar Panels

- Finding the total energy for solar

- Finding Solar Panel size, based on the number of time/ hours of Sunlight

- Finding Battery size

- Finding the size of Solar Charge Controller

- Finding Inverter Size

Solar panels can be easily deployed both in on and off-grid systems. Batteries provide backup to the system and depends on the use of the sytem the time required to run the batteries actually if we increase the size of the batteries than backup time is extended and also if we increase the amount of solar panels than we also have more power source to charge the batteries quickly for longer use , actually more solar panels are required for areas where there is less sunlight than normal daylight conditions, also for remote areas where there is no supply of electricity such as Bajaur, Dir, Dikhan,Bannu these are areas where there is less or no electricity supply, such areas are better for solar installation to decrease costs and maintenace problems of sites .Site will be always on air and there will be no connectivity issue as continous power is available to BTS. There are usually two types of batteries

- Lead acid batteries that are rechargeable batteries with different potential differences.

- Dry batteries that are also rechargeable and include lithium, alkaline and silver oxide batteries

The payback period of solar is not more than five years

C. Diesel Generator sets

Normally a diesel generator working load varies from 5 KVA to 500 KVA , also we know that for an ideal case power factor is 1, than if we assume that power factor is 0.8 than we can easily convert real power or active power to apparent power by formula.\ KVA=$\frac{KW}{PowerFactor}$, so for 8 KW we have KVA=$\frac{8}{0.8}$ = 10 apparent power also if the load increases oil intake of generators also increases. To calculate the units consumed in 1 hour than 1 x 8 KW = 8 KWH. 1 liter of diesel is equivalent to 0.84 KG or 0.8 KG round than, if a diesel consumes 10 KGs of oil than it is equivalent to $\frac{10}{0.84}$ = 11.90$Liter$.

D. Data collection

To analyze final results we have collected data by using questionnaires and direct interviews. interviews was collected at regional offices of KPK which is place in Peshawar region. To get explained and cleared interviews we have observed about 300 of employees from all companies in very relax mode. Quantitative data was from fresh data base records and receipts. duration of interviews with one person was upto 20 minutes. Targeted companies was expertises in installation of solar panel and their power feed back.

E. Interview Responses

Response of employee was in good,relax mode and understandable. some of the questions which was asked during interviews are mentioned below.

Q1) What is the payback period of these solar power systems installed by SPT? Answer: Although the initial cost of these systems is high but it is one time investment and all the systems are exempt from the monthly or yearly bills. Hence, the money that is invested on these systems can be returned back within few months or years depending upon the type of system being installed. Beside this, there is no maintenance cost and for each system; the company also offers the warrantee. The cost analysis has been done to find out payback period of each system mathematically.

Q2: Do you think solar energy technology is the best option in the present energy situation of Pakistan? If yes, can you justify your answer? Answer: Yes indeed, solar energy is the best alternative technology that can be used in the present energy situation of Pakistan. There are many factors that strongly support the implementation of solar energy in Pakistan. These are as follows:

- Pakistan is ranked at position 6th throughout the world for receiving high solar radiations.[14]

- In most part of the country, the sun shines for an average of 3000 hours/year.

- The provinces of Punjab, Sindh and Baluchistan receives approximately 2500 KWh of solar radiation per square meter for one year, while Khyber Pakhtun khwa receives approximately 2200 KWh of solar radiation per square meter for one year[15].

- 7000 mega joules of solar energy are being wasted every year, which can be otherwise efficiently utilized in order to minimize the energy shortfall.

Q3: Share your views about the promotion of these solar technologies in Pakistan over the recent years? Answer: These improvements are as follows:

- Availability of a wide range of solar products.

- Prices of solar products have declined from 2009 onwards, due to expansion in its sales market.

- Conventional tube wells are upgraded to solar energy that saves a lot of power to the national grid.

- Water heather have also been upgraded to solar system which is also a source to save energy.

Q4: As a sales manager of the Solar Power Traders what are the main needs of the people? Answer: The needs of people are mainly regarding the solar home off grid systems, solar water pumps and the solar water heaters.

F. Method of Analysis

Remote areas BTS gensets data was gathered from Mobilink employees, cluster and site engineers the data contains remote areas NORTH2 region activity report and daily activity plan in Microsoft excel, fuel cost was calculated for different sites in NORTH2, also a simulation was implemented using a schematic BTS load, Grid, PV(2KW,3KW), GENSETS(8KVA,12KVA), Converter and Batteries in Homer pro micro grid analysis tool. PODS 16 rectifiers usage and its deployment with alternate energy sources like solar was carefully analyzed to get the results.

IV. ANALYSIS

TABLE I.   SOLAR AND GENSETS MAINTENANCE COSTS FOR ONE MONTH

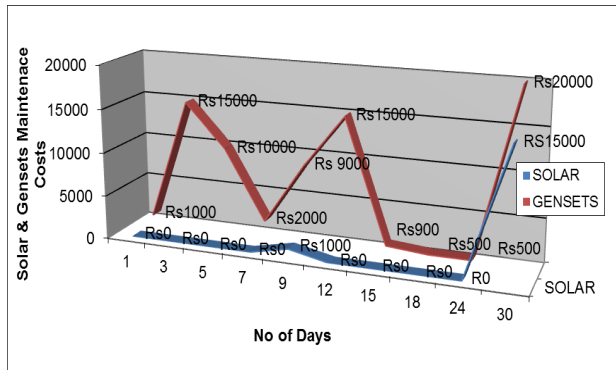| No. of Days	Solar & Genset Maintenance Cost	
S.no	Solar	Gensets
1	0	1000
3	0	15000
5	0	10000
7	0	2000
9	1000	9000
12	0	15000
15	0	900
18	0	500
24	0	500
30	15000	20000

Fig. 1.   Solar and Gensets maintenance cost

V.   FUEL COSTS COMPARISONS FOR GENSETS

As we know that the updated price of diesel is Rupees. 83.79, so for taking a remote area BTS site of DI-KHAN 1,848 liters of diesel is consumed in 55 hours duration as the benchmark of diesel generator for this site is 1.4 liters per hour so Rupees 1,54,844 is spent, on the other side in solar no fuel cost is needed as solar panel takes power from direct sunlight. The simulation results of solar and gensets is also shown in the figure.

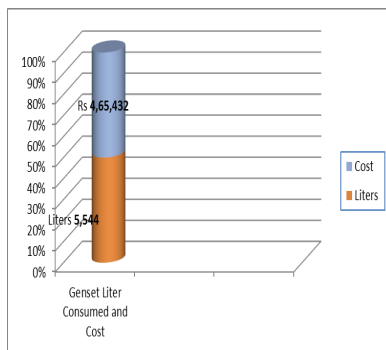| DIESEL GENSET FUEL COSTS FOR THREE DAYS	
FUEL	COST
Liters 1848	Rs 1,54,844

Fig. 2.   Diesel gensets fuel costs for three days

For DI-KHAN site genset operating for ten days will cost round about Rupees 4,65,432 and fuel consumed in liters is 5,544, whereas on the other hand solar is free of cost on the basis of fuel, also a simulation is also carried out in the homer pro.

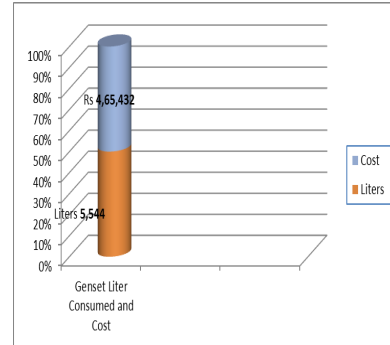| DIESEL GENSET FUEL COSTS FOR TEN DAYS	
FUEL	COST
Liters 5544	Rs 4,65,432

Fig. 3.   Diesel gensets fuel costs for ten days

For DI-KHAN site genset operating for 30 days, or one month will cost round about Rupees 13,93,596 and fuel consumed in liters is16,632, whereas on the other hand solar is free of cost on the basis of fuel.

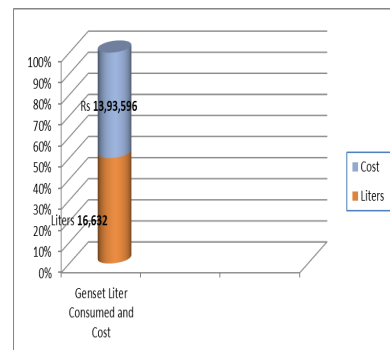| DIESEL GENSET FUEL COSTS FOR THIRTY DAYS	
FUEL	COST
Liters 16,632	Rs 13,93,596

Fig. 4.   Diesel gensets fuel costs for thirty days

For DI-KHAN site genset operating for 365 days, or one year will cost round about Rupees 1,67,23,143 and fuel consumed in liters is1,99,584, whereas on the other hand solar is free of cost on the basis of fuel.

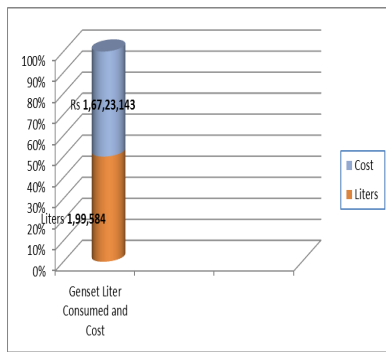| DIESEL GENSET FUEL COSTS FOR ONE YEAR	
FUEL	COST
Liters 1,99,584	Rs 1,67,23,143

Fig. 5.   Diesel gensets fuel costs for one year

A. Sensitivity Analysis

You can use many inputs in order to find different variations in results using a powerful tool homer. These multi input variables are called the sensitivity variables. These sensitivity variables are likely to help the user to cover different inputs on a system and help to find out uncertainty in a system. These sensitivity variables are used for hourly, and monthly data sets of electric load.

B. Hybrid Power Analysis

Different power sources ,hydro, wind energy and solar can be easily deployed to a system and its net effect on the system can be easily derived from it on the basis of cost and other performance parameters.

C. Optimization Analysis of Power Gensets and Comparison with Solar

Model analysis on the basis of different possible results are achieved using homer as a simulation tool, by varying the number of batteries, solar, size of converter, costs and other decision variables.

D. Scaling Process

Scaling process is necessary to find out the total magnitude of the load data with an option that dosent changes the daily load.

VI.   HOMER SIMULATION RESULTS

The results of homer simulation are as follow.

TABLE II.   HOMER SIMULATION RESULTS OF DI-KHAN SITE

Project Location	
Location	DI-Khan Pakistan
Latitude	66 Degrees 34.24 minutes north
Longitude	19 Degrees 57.07 minutes west
Time Zone	Etc/GMT

This graph shows us per kilo watt hour use of gensets used for DI-Khan area, the calculation used depicts homer simulation results for 10KVA and 20KVA per one day usage.

TABLE III.   LOAD ANALYSIS

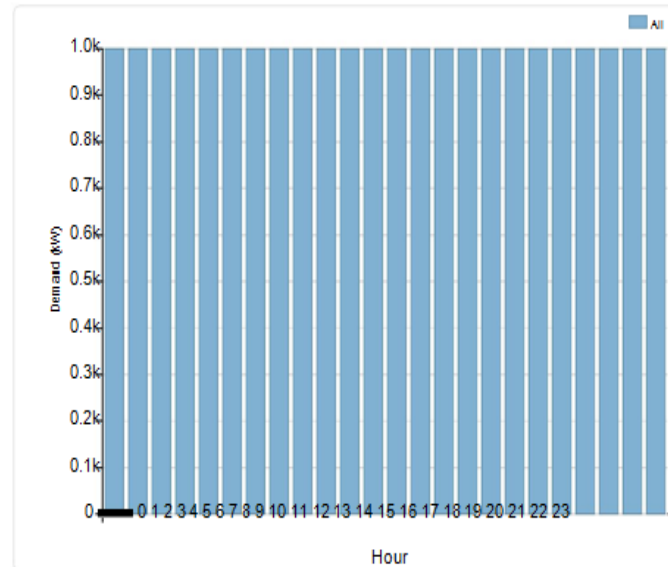| Load	
Data source	Synthetic
Daily noise	10%
Hourly noise	20%
Scaled annual average	24,000.000 KWh/d
Scaled peak load	1,833.2300 KW
Load factor	0.5455

Fig. 6.   Diesel gensets per kilo watthour demand

TABLE IV.   PHOTOVOLTAIC CELLS SIZE AND COST

PV Generic Flat plate PV			
Size	Capital	Replacement	O&M
2KW	Rs300,0000	Rs30,000	Rs18,900
3KW	Rs410,000	Rs42,000	Rs30,240

TABLE V.   SOLAR SPECIFICATION IN HOMER USED FOR ANALYSIS

Solar Resource	
Sizes to consider	2&3KW
Scaled annual average	$5.14 \text{ kWh/m}^2/d$
Lifetime	25 year
Derating factor	80%
Tracking system	Horizontal axis, monthly adjustment
Slope	66.571 deg
Azimuth	0.651 deg
Ground reflectance	20.0%

TABLE VI.   GENSETS SPECIFICATION ANALYSIS USED IN HOMER SIMULATION

Generator:10KVA&20KVA	
Sizes to consider	12&15
Scaled annual average	15,000 hours
Lifetime	15,000hrs
Min load ratio	25%
Heat recovery ratio	39%
Fuel used	Diesel
Fuel curve intercept	0.0480 L/hr/kW
Fuel curve slope	0.2860 L/hr/kW
Diesel cost per liter	Rs 83.40/L
Lower heat value	43.2 MJ/Kg/m^3
Carbon content	88.0%
Sulfur Content	0.3%
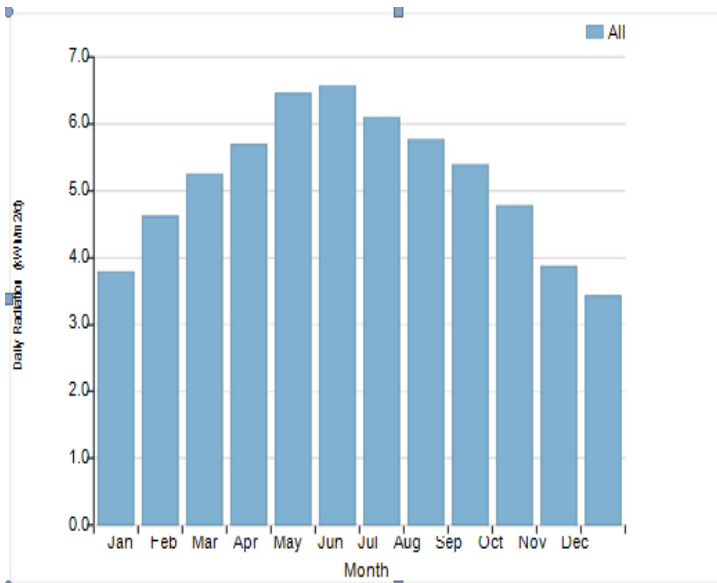
Fig. 7.   Solar usage and performance
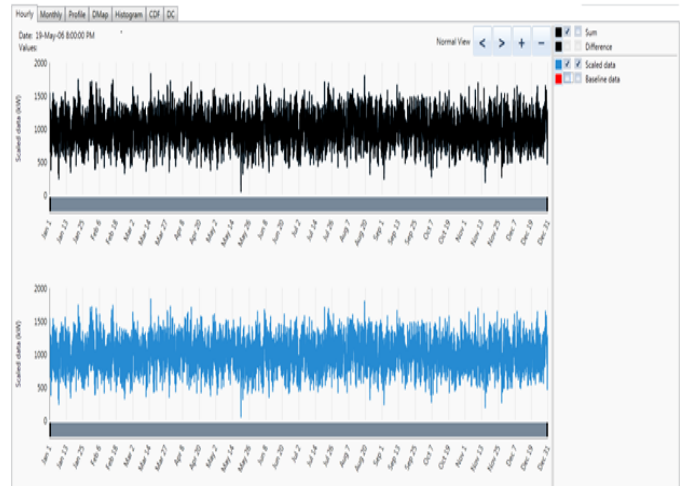
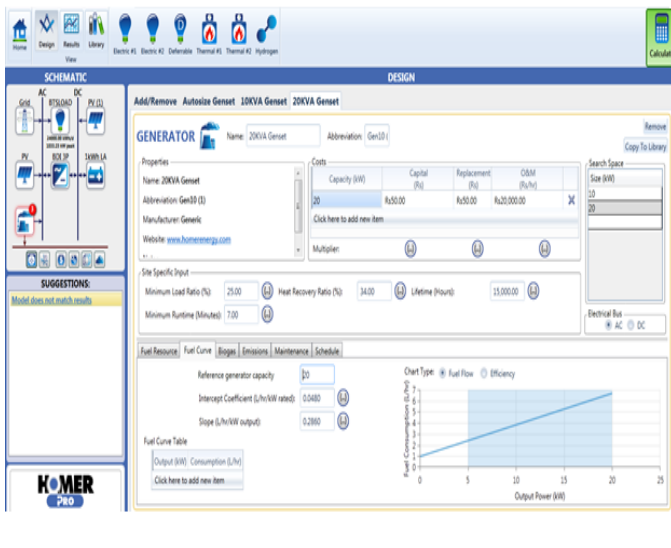Fig. 9.   comparison of solar and gensets during BTS load(site on air)

TABLE VII.   OVERALL HOMER SIMULATION SYSTEM CONTROL TABLE

System Control	
Check load following	YES
Check cycle charging	YES
Setpoint state of charge	80
Allow system with multiple generators	YES
Allow multiple PV cells to operate simultaneously	YES
Allow system with generator capacity less than the peak load	YES
Maximum annual capacity shortage	80
Minimum renewable fraction	8
Operating reserve as percentage of hourly load	20
Operating reserve as percentage of solar power output	85
Operating reserve as percentage of peak load	30

Fig. 8.   Diesel gensets fuel costs and scaled usage results

Battery(1kwh lead acid)	
Quantities to consider	320,550
Voltage	12V
Nominal capacity	83Ah
Lifetime throughput	[800]kWh

Converter	
Quantities to consider	125,0kW
Lifetime	10yr
Inverter can parralel with AC generator	YES
Lifetime throughput	[800]kWh

VII.   RESULTS

On the basis of the above comparisons I prefer solar to be installed on BTS and replace genset as it is costly because of its fuel consumption and maintenance. Apart from cost genset is harmful for environment as its smoke contains chemicals harmful for environment and on the other side solar is environmental friendly. Other important factor is that taking fuel to remote areas is quite difficult and maintenance team became exhausted as it has to take fuel to remote areas of our country.

VIII.   CONCLUSION

On behalf of the total data gathered and to the point meaning of that is that comparisons results of both solar and gensets have been studied, cost of solar and gensets have been compared, total data gathered from Mobilink north2 region sites have been categorized on the basis of activity plan and activity report. Rough assessment of solar and its installation on behalf of the new LTE equipment of power that is the power on distribution (PODS) 16 rectifier have been discussed to show that solar can take t-prime or use T-prime for BTS instead of the gensets as it is costly especially for remote areas sites of the mobilink company.

IX. FUTURE WORK

This research can further be extended by adding all areas of Pakistan such as North-I, Center-I, Center-II. Telecommunication sector in Pakistan is divided into these four regions in which we have worked out for only North-II region Remote areas. We examine cost and performance analysis for solar photo voltaic system vs. gensets for targeted region.so the future work area of this research is directed to analyze for remaining three regions.

—

REFERENCES

[1] Brown, Eric. William. (1988). An introduction to solar energy. College of Computer and Information Science. Feneric. Published

[2] Abdul Waheed bhutto, Aqeel Ahmad Bazmi, and Gholamreza Zahedi, 2011. Greener energy: Issues and challenges for PakistanSolar energy prospective. Renewable and Sustainable Energy Reviews. Published

[3] title=Realization of a near-perfect antireflection coating for silicon solar energy utilization, author=Kuo, Mei-Ling and Poxson, David J and Kim, Yong Sung and Mont, Frank W and Kim, Jong Kyu and Schubert, E Fred and Lin, Shawn-Yu, journal=Optics letters, volume=33, number=21, pages=2527–2529, year=2008, publisher=Optical Society of America. Published

[4] Sealite, The benefits of solar power, s.l.: s.n. in press

[5] Harry Husted, 2010. Solar energy and its use today. published

[6] Zulfiqar Ali,July 2013. KP people find solace in solar energy, Peshawar: DAWN.com. Anon., 2010. [Online] Available at: http://www.valopia.com/index.php/pdf/Solar/solar-energy-advantages-benefits-a-disadvantages.pdf .Published

[7] Mark Sauders, 2015. Research Methods for business students. Harlow: Pearson. Book

[8] Syed Turab Hussain, 2014. Pakistans Energy Sector Issues: Energy Efficiency and Energy. The Lahore Journal of Economics. Published

[9] Hassan Nawab,30th Jan 2013. Energy situation in Pakistan, Islamabad: s.n.

[10] SUNTECH, 2013. SUNTECH COLLABORATES WITH AEDB TO DELIVER SOLAR TO PAKISTAN, Beijing: s.n. Traders, S. P., 2013. For a bright and clean future. [Online] Available at: http://www.solarpower.com.pk/aboutus.php [Accessed 22 july 2013]. Website

[11] Lawrence Neuman James, 2015. Social Research Methods. Boston: Pearson Education, Inc. Book

[12] Umar Khan Mirza, Maroto-Valer, Mercedes Maroto-Valer. and Nasir Ahmad, 2003. Status and outlook of solar energy use. Elsevier. Published

[13] title=Critical success factors for successful lean Six Sigma implementation in Pakistan, author=Zhang, Qun and Irfan, Muhammad and Khattak, M and Abbas, Jaffar and Xiaoning, Z and Shah, M, journal=Interdisciplinary Journal 0f Contemporary Research In Business, volume=4, number=1, pages=p117–124, year=2012. Published

[14] Qazi Nauman, Zahid, 2015. MARKET ENTRY MODE FOR SOLAR AND WIND ENERGY BASED ON MARKET ANALYSIS FOR PROSPECTIVE FINNISH COMPANIES, Published

[15] Nadeem, Mukhtar, Hayat, and Rafique, 2015. Power sector- An overview